

AD-A015 989

HOLOGRAPHIC LENS FOR PILOT'S HEAD-UP DISPLAY

Donald H. Close, et al

Hughes Research Laboratories  
Malibu, California

1 April 1975

DISTRIBUTED BY:

**NTIS**

National Technical Information Service  
U. S. DEPARTMENT OF COMMERCE

# HOLOGRAPHIC LENS FOR PILOT'S HEAD-UP DISPLAY - PHASE 2

ADA 015989

D. H. CLOSE, A. AU, AND A. GRAUBE

HUGHES RESEARCH LABORATORIES  
3011 MALIBU CANYON ROAD  
MALIBU, CA 90265

1 APRIL 1975

CONTRACT N62269-74-C-0642  
FINAL TECHNICAL REPORT  
FOR PERIOD 1 JULY 1974 - 31 OCTOBER 1974

APPROVED FOR PUBLIC RELEASE; DISTRIBUTION UNLIMITED.

PREPARED FOR

NAVAL AIR DEVELOPMENT CENTER  
WARMINSTER, PA 18974

DDC  
RECEIVED  
OCT 17 1975  
REGISTRATION  
B

Reproduced by  
NATIONAL TECHNICAL  
INFORMATION SERVICE  
U.S. Department of Commerce  
Springfield, VA 22151

UNCLASSIFIED

SECURITY CLASSIFICATION OF THIS PAGE (When Data Entered)

REPORT DOCUMENTATION PAGE		READ INSTRUCTIONS BEFORE COMPLETING FORM	
1. REPORT NUMBER N62269-74-C-0642	2. GOVT ACCESSION NO. NADC-75044-30	3. RECIPIENT'S CATALOG NUMBER	
4. TITLE (and Subtitle) HOLOGRAPHIC LENS FOR PILOT'S HEAD-UP DISPLAY - PHASE II	5. TYPE OF REPORT & PERIOD COVERED Final Technical Report 1 July 1974-31 October 1974	6. PERFORMING ORG. REPORT NUMBER	
7. AUTHOR(s) D.H. Close, A. Au, and A. Graube	8. CONTRACT OR GRANT NUMBER(s) N62269-74-C-0642	9. PERFORMING ORGANIZATION NAME AND ADDRESS Hughes Research Laboratories 3011 Malibu Canyon Road Malibu, California 90265	10. PROGRAM ELEMENT, PROJECT, TASK AREA & WORK UNIT NUMBERS
11. CONTROLLING OFFICE NAME AND ADDRESS Naval Air Development Center Warminster, PA 18974	12. REPORT DATE 1 April 1975	13. NUMBER OF PAGES 59	14. MONITORING AGENCY NAME & ADDRESS (if different from Controlling Office)
	15. SECURITY CLASS (of this report) UNCLASSIFIED	15a. DECLASSIFICATION-DOWNGRADING SCHEDULE	
16. DISTRIBUTION STATEMENT (of this Report) Approved for public release, distribution unlimited			
17. DISTRIBUTION STATEMENT (of the abstract entered in Block 20, if different from Report)			
18. SUPPLEMENTARY NOTES			
19. KEY WORDS (Continue on reverse side if necessary and identify by block number)			
Head-Up Display		Fringe Control System	
Hologram Recording Apparatus		Acoustic Shield	
Construction Beam Optical System		Fringe Stability	
Vibration Isolation		Processing Equipment	
20. ABSTRACT (Continue on reverse side if necessary and identify by block number)			
This report describes work on the development of a hologram recording apparatus with a fringe control system for 16 in. diameter, 50° off-axis, symmetric transmission holographic lens for pilot's Head-Up Display (HUD). The basic HUD system parameters are a 25° field of view, a 25 in. eye relief, and a 3 in. by 5 in. wide exit pupil. The hologram geometry was chosen based on parametric analysis and preliminary studies on several Hughes continuous reflection and			

**DDC**  
**RECEIVED**  
**OCT 17 1975**  
**REGULATORY**  
**B**

UNCLASSIFIED

SECURITY CLASSIFICATION OF THIS PAGE (When Data Entered)

transmission hologram lens designs of Phase I, Contract N62269-73-C-0388, Holographic Lens for Pilot's Head-Up Display. The work also includes design of processing equipment for large holographic lens elements recorded on 18 in. x 18 in. dye-sensitized dichromated gelatin, holographic plates. 18 in. x 18 in. x 0.25 in. thick photographic plates were procured under this contract.

Based on the 'continuous lens' design approach, the specified construction beams consist of a diverging point source 25 in. from the hologram recording plane and a converging point source image 35 in. behind the hologram recording plane. The normal to the hologram recording plane bisects the 50° included angle of the construction beams. Aberrations in the converging point source image, from a 36 in. diameter, 72 in. radius of curvature spherical mirror, were reduced with two cylindrical correction elements to a spot size of 0.2 in. diameter while keeping irradiance nonuniformity to less than 3% across the hologram aperture.

Fringe stability over the maximum 2 hours exposure on dye-sensitized dichromated gelatin was a primary goal in assembling the construction optics to provide the proper wavefronts to record the hologram optical element. Environmental isolation of the construction beam optical system from normal in-house building vibrations and air-borne disturbances was achieved on a 5 x 10 x 10 in. granite optical table supported by six vibration isolation, pneumatic mounts and an acoustic shield 5 x 9 x 40 in. high. In-house designed construction hardware provided stable mechanical mounting of optical components on optical axes 19-1/4 in. above the granite surface. Evaluation of the completed exposure apparatus showed excellent short term stability where fringe drifts were typically less than a full fringe depth per half hour.

Dramatic improvements on fringe stability was achieved with the design and implementation of an interferometer phase detection system and feedback fringe control electronics. The relative axial phase of the construction beams was monitored from low spatial frequency interference fringes of the axial construction wavefronts. Integrating feedback electronics actively lock the relative axial phase by piezoelectrically translating a plane mirror in the object beam path. Experimental performance evaluation of the fringe controlled exposure apparatus showed  $\lambda/22$  fringe stability maintained for two hours.

Circulation drying chamber and nitrogen burst agitation tanks were designed for uniform processing of 18 in. x 18 in. holographic plates to enhance reproducibility of high quality, uniform large aperture hologram lenses.

UNCLASSIFIED

SECURITY CLASSIFICATION OF THIS PAGE (When Data Entered)

TABLE OF CONTENTS

SECTION		PAGE
	LIST OF ILLUSTRATIONS . . . . .	4
	PREFACE . . . . .	7
I	INTRODUCTION AND SUMMARY . . . . .	8
II	CONSTRUCTION BEAM OPTICAL SYSTEM . . . . .	18
III	ENVIRONMENTAL ISOLATION . . . . .	28
IV	FRINGE CONTROL SYSTEM . . . . .	38
V	PERFORMANCE . . . . .	48
VI	PROCESSING EQUIPMENT DESIGN . . . . .	56
	REFERENCES . . . . .	59

## LIST OF ILLUSTRATIONS

FIGURE		PAGE
1	(a) Vertical section of the NADC 50° off-axis, symmetric transmission HUD system . . . . .	19
1	(b) Point source construction beams of the NADC 50° off-axis, symmetric transmission HUD system . . . . .	19
2	50° off-axis, symmetric transmission hologram aperture required for a 25° circular FOV . . . . .	19
3	(a) Object beam numerical aperture requirement . . . . .	21
3	(b) Reference beam numerical aperture requirement . . . . .	21
4	HUD hologram construction beam optical layout with aberration correction cylindrical lenses in the reference beam . . . . .	23
5	(a) Computer ray trace data of geometric aberration in the corrected reference point source image . . . . .	25
5	(b) Aberrations in the reference point source image were reduced to a blur size of less than 0.2 in. . . . .	25
6	Irradiance variation in the reference beam across the hologram aperture reduced to less than 33% . . . . .	27
7	Spatial frequency of 1306 fringe cycles per millimeter is recorded in 50° off-axis, transmission hologram . . . . .	29
8	Low resonance frequency pneumatic isolation mounts . . . . .	31
9	First order bending mode at 115 Hz and torsional bending mode at 142 Hz . . . . .	31
10	Vertical translators with support posts provide stable mechanical mounting of construction optic . . . . .	33

FIGURE		PAGE
11	Interferometer mount with interconnecting supports and 18 in. square holographic plate holder . . . . .	34
12	36 in. diameter, 72 in. radius of curvature spherical mirror is mounted vertically . . . . .	35
13	Cylindrical correction element mounts . . . . .	35
14	Cross-section material sketch of acoustic enclosure . . . . .	37
15	Phase perturbation during exposure of a hologram causes reduction of recorded fringe contrast . . . . .	39
16	Interferometer system expands the relative axial fringe at the hologram recording plane . . . . .	41
17	Two identical, 180° out of phase, low spatial frequency interference patterns are formed . . . . .	43
18	A 200 mm f.l. positive achromat converges the diverging object beam . . . . .	45
19	Optical layout of the interferometer system . . . . .	45
20	Feedback electronic corrects axial phase instability by translating a plane mirror in the object beam . . . . .	47
21	Full-scale, 50° off-axis, symmetric transmission hologram lens recording system . . . . .	49
22	Full fringe depth corresponding to a $\lambda/2$ relative path length shift . . . . .	51
23	Vibration isolation, pneumatic mounts improve fringe stability by 10 times . . . . .	51
24	High frequency acoustical noise at 120 Hz, the first torsional bending frequency of the graphite surface, is attenuated by the acoustic shield . . . . .	52

FIGURE		PAGE
25	Experimental evaluation of the full-scale hologram recording apparatus without fringe control exhibits good short term stability . . . . .	53
26	Low amplifier noise, with no input . . . . .	55
27	Experimental evaluation of the full-scale recording system show that $\lambda/22$ fringe stability for two hours is maintained by the active fringe control system . . . . .	55
28	Drying chamber designed to ensure uniform drying of 18 in. x 18 in. holographic plates . . . . .	57
29	Processing tank table with nitrogen-burst agitation tanks . . . . .	57

## PREFACE

This final report covers the work accomplished during the period 1 July 1974 through 31 October 1974 under Contract Nb2269-74-C-0642, "Holographic Lens for Pilot's Head-Up Display (Phase 2)." This work was supported by the Naval Air Systems Command under the sponsorship of Mr. George Tsaparas and Mr. William B. King. The program is under the technical direction of Mr. Ed Rickner, Mr. Ken Priest and Mr. Harold Green of the Naval Air Development Center, Warminster, Pennsylvania.

The work was accomplished by the Exploratory Studies Department of the Hughes Research Laboratories Division of the Hughes Aircraft Company, under the direction of Dr. Donald H. Close. The technical work was performed by Mr. Anson Au, with the able assistance of Mr. Cesar C. De Anda, who did much of the mechanical design and performed many of the experiments. Other contributors were Mr. Andrejs Graube, who provided the processing equipment design, and Mr. John F. Belsher, of the Electro-Optics Department, who provided the reference beam optical system design and specification. Mr. Gaylord E. Moss acted as a consultant to the program and provided valuable assistance in the conduct of all major tasks.

## I. Introduction and Summary

### 1. INTRODUCTION

This final technical report contains a detailed discussion of the Phase 2 NADC program tasks, objectives, approaches and results toward developing a Holographic Lens for Pilot's Head-Up Display.

This is the final technical report on Contract N62269-74-C-0642, Phase 2 of the Naval Air Development Center (NADC) program to develop a Holographic Lens for Pilot's Head-Up Display (HUD). The work covered by this report was performed at Hughes Research Laboratories, Malibu, California during the period 1 July 1974 to 31 October 1974.

The NADC program is to develop a HUD system meeting the optical system parameters and performance goals as stated in the NADC "Specification for Hologram Lens System."<sup>1</sup> The basic system parameters are a 25° field of view (FOV), an exit pupil size of 3 in. high by 5 in. wide, and an eye relief of 23 in. As a result of the favorable results of the Phase 1 program,<sup>2</sup> in which preliminary system design and recording material optimization led to a demonstration of high quality holographic HUD imagery in a half-size transmission hologram element with an off-axis angle of 40°, we recommended a transmission hologram configuration with an off-axis angle of 50° for the next phase of technology development, although the final system may not have the same configuration.

Because the basic system constitutes a high quality, off-axis eye-piece covering a FOV of 25° from any point within the exit pupil, a hologram element of 16 in. diameter is required to meet the "Specifications for Hologram Lens System." This represents major technological steps in constructing and processing large holographic optical elements.

Phase 2 of this program, the specific subject of this technical report, covers the design and fabrication of the apparatus capable of the large hologram fabrication. Table 1 outlines the Tasks, Objectives, Approach and Results of the Phase 2 program. A delay in the completion of Phase 2 was caused by vendors' delays on delivery of large optics used in the construction beams of the recording apparatus. However, the successful completion of the Phase 2 tasks is a big step toward successful development of a high quality holographic HUD system. Although the tasks in Phase 2 were performed with the recommended transmission configuration in mind, a changeover to a reflection configuration is feasible. The ability to fabricate a large transmission hologram lens, although it may not be the final system configuration, is a big technological step in the state of the art of HUD design and fabrication.

TABLE I

TASK	OBJECTIVES	APPROACH	RESULTS	LOCATION
1. Full-scale hologram construction optics design and assembly	Design and fabricate recording apparatus for 50 off-axis, symmetric transmission hologram lens which meets the basic MDC system parameters.	Procure optics to meet construction beam design specifications; computer based aberration correction optics; stable construction hardware design	Assembled full-scale hologram recording apparatus provides the proper point source construction beams for 14 5/8" focal length hologram and lens	Section III(1-4) Section III(13) Section VIII
2. Environmental Isolation	Provide environmental isolation of recording apparatus from mechanical and airborne disturbances.	5 ft x 10 ft x 10 in. thick granite optical table with six piezoelectric supports, 7 ft x 9 ft by 40 in. high acoustic and environmental shield	Optical table provided a 1% fringe movement in fringe stability; acoustic shield provided high attenuation of air turbulence and acoustic noise 100 dB	Section III(13) Section VIII
3. Fringe control system design and assembly	Design and fabricate feedback fringe control system to lock the relative axial phase of the construction beams to within $\pm 10$ .	Interferometry phase detection with feedback control electronics with a PZT transducer to actively correct relative phase errors.	Relative axial phase of construction beam is detected and locked in by interferometry feedback control system; translating a mirror in the object beam	Section VIII-45
4. Fringe stability evaluation	Maintain fringe stability of $\pm 10$ in the recording apparatus with environmental isolation and fringe control system for 1-2 hours exposure period.	Evaluate recording apparatus system performance by taking fringe stability measurements using a HeNe laser at 632.8 nm	Less than two hours fringe stability of $\pm 2$ attained with the fringe control system.	Section V(1)
5. Processing equipment design	Design processing equipment suitable for uniform and reproducible processing of full-scale holograms in dye-sensitized dichromated gelatin.	Highly controlled drying stage, nitrogen burst agitation tank.	Drying chamber and agitation tank designed for high quality processing of 11 x 18" hologram recordings.	Section VIII
6. Photographic plates procurement	Procure large photographic plates suitable for full-scale hologram recordings.	18 in. x 18 in. x 0.25 in. Kodak 649F and 120-01 photographic plates.	36-649F and 36-120/01 Kodak photographic plates procured and received.	

1. Introduction and Summary
2. SPECIFIED SYSTEM PARAMETERS AND PERFORMANCE GOALS

The optical characteristics specified by the NADC "Specification for Hologram Lens System" are a 25° field of view, a 25 in. eye relief, a 3 in. high by 5 in. wide exit pupil, and high quality imagery.

The basic system characteristics as specified by the NADC "Specification for Hologram Lens System" are summarized in Table 2 along with the performance goals. The major parameters are a 25° circular FOV, a 25 in. eye relief, and an operating wavelength of 632.8 nm (HeNe Laser). An acousto-optical laser scanning system provides the input to the display system on a 4 in. x 4 in. diffusing screen. In order to provide a 25° FOV from this source, the system focal length must be

$$f_o = \frac{4 \text{ in.}}{2 \tan 12.5^\circ} = 9.0 \text{ in.}$$

Taking the 25 in. eye relief, 3 in. high by 5 in. wide exit pupil, and the vertical tilt of the hologram element, the size of the hologram element is approximately 16 in. diameter. Only the thin film, low weight nature of hologram optical elements makes it feasible to consider such a large size HUD lens.

The "continuous lens" design approach,<sup>3</sup> invented at Hughes Research Laboratories by Mr. Gaylord Moss, provides high optical efficiency across the angular FOV, and has uniform correctable aberrations. The performance goals summarized in Table 2, are applicable to both transmission and reflection hologram optical elements in the HUD system. Although either a reflection or a transmission geometry can be designed to meet the system specification, the overall image quality and efficiency characteristics are better for a transmission system than for corresponding reflection system. Also, because of fabrication ease in practice, a transmission system which meets the "Specification for Hologram Lens System" was recommended for this phase of technological development.

TABLE 2

## 25° Field of View System

Given Parameters	
Field of View	25° circular
Eye Relief	25 in.
Exit Pupil Size	3 in. high x 5 in. wide
Operating Wavelength	632.8 nm (monochromatic)
Calculated Parameters	
Hologram Size	16 in. x 16 in.
System Focal Length	9.0 in.
Performance Goals	
Optical Efficiency	80% min
Resolution	1.0 mrad
Accuracy	1.0 mrad, central 12° 2.0 mrad, to 25°
Binocular Disparity	
Vertical	Less than 1.0 mrad
Horizontal divergent	Less than 1.0 mrad
Horizontal convergent	Less than 2.5 mrad

T1373

I. Introduction and Summary

3. RECOMMENDED SYSTEM GEOMETRY

The parametric analysis performed during the Phase 1 program led to the recommendation of a transmission hologram configuration with an off-axis angle of  $50^\circ$  for the Phase 2 construction of a recording apparatus with fringe control system, and design of processing equipment.

Based on the results of the parametric study performed in Phase 1 and on the current state of the art of hologram lens design and fabrication, a symmetric transmission hologram with an off-axis angle of  $50^\circ$  complying with the NADC "Specification for Hologram Lens System" was chosen for this phase of technological development. A hologram element size of 16 in. diameter is necessary to obtain the  $25^\circ$  FOV at any point in a 3 in. high by 5 in. wide exit pupil. The system focal length must be 9 in. in order to provide  $25^\circ$  FOV from the 4 in. square diffusing screen source of the acousto-optical laser scanner. The fundamental requirements of uniform brightness across the  $25^\circ$  FOV, limited length, and exit pupil size, restricted the practical hologram focal length approximately to  $11.25 \text{ in.} < f_h < 14.4 \text{ in.}$ , which correspond to relay lens magnifications in the range of  $1.25 < m < 1.6$ .

Parametric study of overall image quality and efficiency between similar transmission and reflection configurations led to the recommendation of a transmission hologram configuration for constructing the recording apparatus and fringe control system. Another factor in the choice of a transmission configuration was the fabrication ease compared to a reflection geometry, due to lower requirements for large area fringe stability and large area material thickness uniformity. The system characteristics corresponding to the geometry of the Phase 2 recording apparatus are shown in Table 3. This may not be the final system configuration, depending on the correctability of spectral flares visible in the FOV, due to diffraction of sunlight. However, the experience, equipment, and technology produced by the Phase 2 program can be applied to whatever configuration is ultimately chosen.

TABLE 3

HOLOGRAM CHARACTERISTICS

Hologram Configuration . . . . . Symmetric transmission  
50° off-axis angle

Hologram Focal Length . . . . . 14.58 in.

SYSTEM CHARACTERISTICS

Relay Lens Basic Focal Length . . . . 7.79 in.

Relay Lens f# . . . . . 1.11

Unfolded Length . . . . . 47.6 in.

I. Introduction and Summary

4. APPLICATION OF PHASE 2 TASKS TOWARD FINAL HUD CONFIGURATION

The experience, equipment and technology covered by this Phase 2 technical report can be applied to whatever ultimate hologram element configuration is chosen to meet the NADC "Specifications for Hologram Lens System."

Although Phase 2 tasks were completed to fabricate the recommended transmission hologram with a  $50^\circ$  off axis angle, the experience, equipment, and technology development covered by this technical report are applicable to whatever geometry is chosen for the final system. One of the Phase 2 tasks covers the design and construction of a full-scale, fringe-stabilized exposure apparatus required for fabrication of the recommended transmission hologram optical element which meets the NADC "Specifications for Hologram Lens System." The "continuous lens" approach, as applied to developing the NADC HUD, allows the holographic optical element to be produced with a single exposure using two point sources. The specifications of the hologram lens element determined the recording beam requirements of the exposure apparatus. This Phase 2 technical report covers the construction beams and construction optics design toward the full-scale symmetric transmission hologram with a  $50^\circ$  off axis angle. Basically, the recording beams consist of a diverging point source 25 in. from the hologram, providing the 25 in. eye relief, and a source converging to a point 35 in. behind the hologram to obtain a focal length of 14.58 in. The  $50^\circ$  off-axis defines the included angle between recording beams. The hologram normal bisects the off-axis angle, producing the symmetrical configuration. Fringe stability was obtained through a phase-comparing interferometer behind the hologram. This interferometer consists of beam-shaping optics to produce low spatial frequency interference patterns, and a servo feedback system which actively modulates the relative phase of the construction beams. Further details of the construction beams and fringe stabilizing system design and implementation will be discussed in this report. Remaining tasks of the Phase 2 program, covered by this report, were the procurement of large photographic plates suitable for recording hologram and full scale hologram processing equipment and design.

Phase or fringe stability during exposure is necessary regardless of the hologram geometry, although reflection geometries, as opposed to transmission geometries, require a higher degree of fringe stability during exposure due to the recorded fringe orientation with respect to the hologram emulsion plane. A reflection hologram with a  $50^\circ$  off-axis angle would be recorded in the construction beams described in this technical report if the hologram plane was rotated  $90^\circ$  so that the

recording beams exposed opposite surface of the holographic plate. Other configurations, both transmission and reflection, can also be constructed if the construction beam's diameter can expose a large enough hologram to obtain a  $25^\circ$  FOV, and if the construction beam's layout does not exceed the surface area of the existing 5 ft x 10 ft granite optical table. An interferometer phase detection system was designed and constructed for the construction beams of the  $50^\circ$  off-axis, transmission hologram. New beam shaping optics may be required for other geometries, although the basic configuration and design of the interferometer system can be applied to any hologram configuration. The feedback control electronics that were designed and fabricated are totally independent of the construction beam geometry. Of major concern in the fabrication of reflection hologram is the additional stability requirement on the holographic plate holder. A careful design study of feasible methods of large holographic plate holding techniques must be done. However, Hughes Aircraft Company has successfully demonstrated the recording of high-efficiency, 2 in. diameter, reflection hologram lenses in developing the Helmet-Mounted Holographic Lens Display for the U. S. Air Force Aerospace Medical Research Laboratory, Wright-Patterson Air Force Base.<sup>4</sup>

Uniform processing is also a basic factor in the successful fabrication of the holographic lens element. The nitrogen gas burst agitating tanks and humidity-controlled drying chamber described in this report can be applied to the processing of large aperture transmission or reflection geometry optical elements. Although the dye-sensitized dichromated gelatin material described in the Phase 1 final report can record both transmission and reflection holographic optical elements, further optimization for large area material thickness uniformity and sealing techniques would be important tasks should a reflection geometry be chosen for future development.

The success of Phase 2 program tasks, which covers the design and fabrication of special apparatus for fabricating the full-scale,  $25^\circ$  FOV, symmetric transmission hologram with  $50^\circ$  off-axis angle, and the expected success in fabricating the full-scale HUD hologram optical element represent a major advancement in the state of the art of hologram lens design and fabrication.

I. Introduction and Summary

5. SUMMARY

The full-scale hologram recording apparatus has been assembled and evaluated with the proper construction beams and long-term fringe control system for high efficiency recording of  $50^\circ$  off-axis symmetric transmission lenses meeting the NADC HUD lens requirements. Processing equipment was designed for uniform processing of 18 in. x 18 in. x 0.25 in. photographic plates, which have been received.

The recording apparatus has been constructed for  $50^\circ$  off-axis, symmetric transmission continuous hologram lenses which meet the NADC specifications for a  $25^\circ$  circular FOV from any point within a 3 in. high by 5 in. wide pupil, and a 25 in. eye relief. The construction beams consist of a diverging point source 25 in. from the center of the hologram and a converging point source image 35 in. behind the center of the hologram. The resultant hologram focal length is 1'.58 in.

The required hologram lens aperture for a  $25^\circ$  circular FOV is +8.32 in. and -7.04 in. in the asymmetric, (vertical) direction and  $\pm 8$  in. in the symmetric (horizontal) direction. The basic construction optics consist of a 20X spatial filter/-50 mm focal length lens combination to meet the 0.30 numerical aperture (NA) requirement of the diverging object beam, and a 36 in. diameter, 72 in. radius of curvature, spherical mirror to meet the 0.22 NA requirement of the converging reference beam. Off-axis aberrations, coma and astigmatism of the large spherical mirror, were reduced by two  $\pm 8.170$  radius of curvature cylindrical lenses, to produce a blur diameter of less than 0.2 in. This blur diameter corresponds to a maximum of 2.86 mrad angular deviation of chief rays from their ideal directions in the system. Irradiance variation across the hologram aperture was reduced to less than 33%. The resultant construction beams exceed the requirements necessary for constructing the specified hologram lens.

The hologram recording apparatus was constructed on a 5 ft x 10 ft x 10 in. thick granite optical table with pneumatic isolation legs which isolated the optical system from mechanical building vibrations, giving a 10 times improvement in fringe stability. A 5 ft x 9 ft x 40 in. high acoustical enclosure, constructed with six lb/ft<sup>3</sup> mineral wool sandwiched between a solid 24 gauge steel outer skin and a 26 gauge perforated steel inner skin, provides good environmental isolation of turbulent air and high attenuation of > 100 Hz acoustical noise. This environmental isolation, along with design and fabrication of stable optical mounts, resulted in a long-term, interference pattern drift rate of typically a full fringe depth per half hour (without feedback stabilization).

Long term fringe control was achieved with a fringe stabilizing system which locks the relative axial phase of the construction beams for at least the maximum required 1 to 2 hour exposure. An interferometer system expands the axial fringe at the hologram recording plane to two  $\pi$  out of phase, low spatial frequency, radial fringes. Feedback electronics integrates the difference phase-related output of the two photodiode fringe detectors, and a piezoelectric mount translates a plane mirror in the object construction beam until the output of the two detectors is balanced. Nine percent or full fringe depth perturbation, i. e., a stability of  $\lambda/22$ , was achieved for 2 hours.

The processing equipment designed for uniform processing of 18 in. square, 0.25 in. thick, dye sensitized dichromated gelatin holographic plates consists of a drying chamber and agitation tanks. A 40% relative humidity chamber with circulating fan ensures uniform drying of sensitized plates. Nitrogen burst agitation tanks were designed to promote uniform swelling and dehydration of the gelatin emulsion. After the agitation processing the hologram can be raised directly into a nitrogen atmosphere chamber, which is fitted over the final agitation tank, without exposure to air and dust. 18 in. x 18 in. x 0.25 in. Kodak 649F and 120-02 photographic plates were procured and are in-house.

## II. Construction Beam Optical Systems

### 1. "CONTINUOUS LENS" CONSTRUCTION BEAM SPECIFICATIONS

Based on the "continuous lens" design approach used to meet system specifications, the construction beams required for a  $50^\circ$  off-axis, symmetric transmission hologram consist of a diverging point source 25 in. from the hologram and a converging point source 35 in. behind the hologram.

The "continuous lens" design approach, described in detail in the Phase 1 technical report, is basically construction beams generated by two point sources which yields high optical efficiency across the angular FOV and has correctable uniform aberrations across the FOV. The Phase 1 final report covered parametric analysis and preliminary system design on various hologram HUD optical elements using the "continuous lens" approach. Either a transmission or reflection geometry hologram lens can be designed to meet system specification, and a transmission configuration was chosen for the Phase 2 development program.

In the "continuous lens" approach, the holographic optical element is constructed with one point source in the center of the system exit pupil, and the other construction point source is located at the image of the system exit pupil formed by the hologram. Based on the system studies and recommended hologram characteristics of the Phase 1 program, a symmetric transmission hologram with a  $50^\circ$  off-axis angle was chosen as the configuration for which the Phase 2 construction beams were designed. A diverging point source located 25 in. away from the hologram, at the center of the 3 in. high by 5 in. wide exit pupil, defines the 25 in. eye relief of the hologram lens HUD system. A converging point source is located 35 in. behind the hologram to give a hologram focal length of 14.58 in. The basic relay lens focal length, determined by the 9 in. system focal length requirement and the hologram focal length, is 7.79 in. The maximum 5 in. exit pupil width determines a required relay lens  $f\#$  of 1.11. The resultant unfolded length of the system from the hologram to the 4 in.<sup>2</sup> diffusing screen input source is 47.6 in. A vertical view of the resulting HUD system is shown in Fig. 1(a) with the corresponding construction beams shown in Fig. 1(b). The overall size of the hologram aperture, shown in Fig. 2, is determined by the system requirement for  $25^\circ$  FOV visibility from any location within the 3 in. high by 5 in. wide pupil.

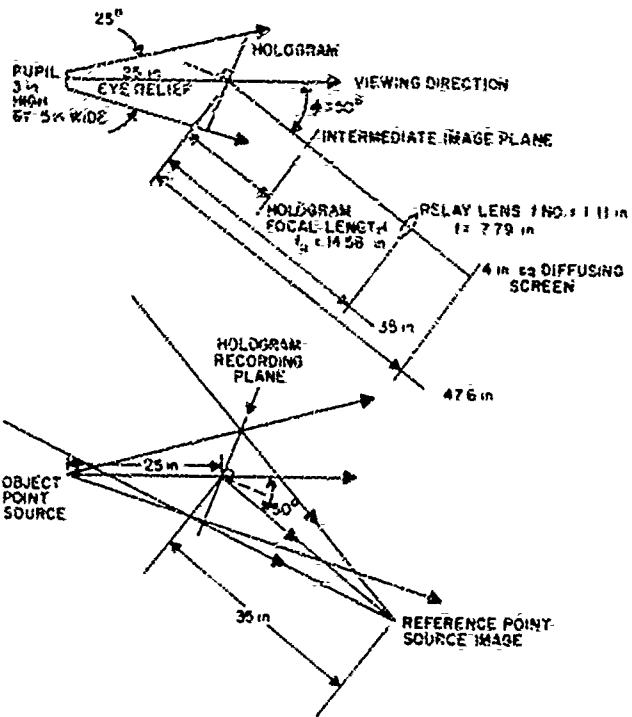


Fig. 1(a).  
Vertical section of the  
NADC 50° off-axis,  
symmetric transmission  
HUD system.

Fig. 1(b).  
Point source construction  
beams of the NADC 50°  
off-axis, symmetric trans-  
mission HUD system.

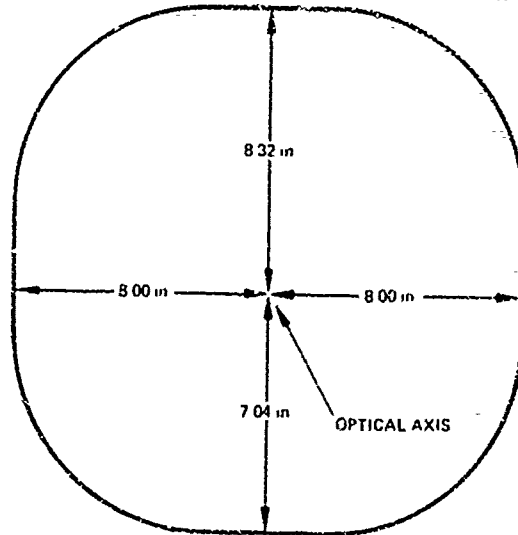


Fig. 2. 50° off-axis, symmetric  
transmission hologram  
aperture required for a  
25° circular FOV.

## II. Construction Beam Optical System

### 2. CONSTRUCTION BEAM OPTICS REQUIREMENTS

A diverging point source, 25 in. from the hologram, with 0.33 numerical aperture, is formed by a 20X spatial filter, -50 mm focal length negative lens combination. A 36 in. diameter, 72 in. radius of curvature spherical mirror forms a 0.23 numerical aperture point source image 35 in. behind the hologram.

A spatially filtered, diverging beam, from a point source 25 in. away from the hologram, and a converging beam, formed by using a 36 in. diameter, 72 in. radius of curvature spherical mirror with two cylindrical correction lenses to produce a point source image 35 in. behind the hologram, form the construction beams. These construction beams are required to fabricate the full scale, symmetric transmission hologram optical element described in Section II-1, which meets the NADC system specifications. The "continuous lens" approach taken describes the location of the two construction beam point source locations, but the hologram aperture required for a 25° FOV determines the numerical aperture of the construction beams and consequently the construction optics size.

The overall aperture required to provide the 25° FOV from any point in the 3 in. high by 5 in. wide exit pupil of the system must be +8.32 in. and -7.04 in. in the asymmetric vertical direction with reference to the optical axis and ±2 in. in the symmetric horizontal direction. With the locations and distances of the construction beam point sources from the hologram determined by the construction beam specifications, a convenient measure of the required beam sizes is the numerical aperture ( $NA = \sin\theta$ , where  $\theta$  is the half cone angle of the beam in air with reference to the optical axis).

A numerical aperture of 0.30 is required in the object beam (the diverging beam) in order to provide a beam diameter large enough to fill the hologram aperture. A 20X spatial filter and a 50 mm focal length, negative lens are used to provide this object beam. Considering only 0.16 NA of the available 0.50 NA of the 20X objective, to ensure uniform intensity by using the top portion of the Gaussian intensity distribution over the 0.50 NA, Fig. 3(a) shows the NA requirements of various sectors of the hologram aperture along with the NA provided by the optics used to provide the object point source. The symmetric horizontal NA are shown in brackets.

A 36 in. diameter, 72 in. radius of curvature spherical mirror reflecting at 30° angle provides the converging point source image 35 in. behind the hologram. Figure 3(b) shows the NA requirements of various sectors of the hologram aperture, along with the NA of the construction beam provided by the 36 in. diameter spherical mirror meeting these requirements. The 36 in. diameter, 72 in. radius of

curvature mirror was manufactured at John H. Ransom Laboratories, Inc. in Los Angeles, California. The mirror was shaped out of a 1-1/4 in. thick pyrex blank to a specified surface quality of 1 fringe per in. and a radius tolerance of  $\pm 1/4$  in. The mirror surface consists of an evaporated aluminum film with a silicon monoxide overcoat. Due to expected delays in delivery of this large optical element, a 14.38 in. diameter mirror with the same characteristics was procured and used to test the apparatus prior to the delivery of the large mirror.

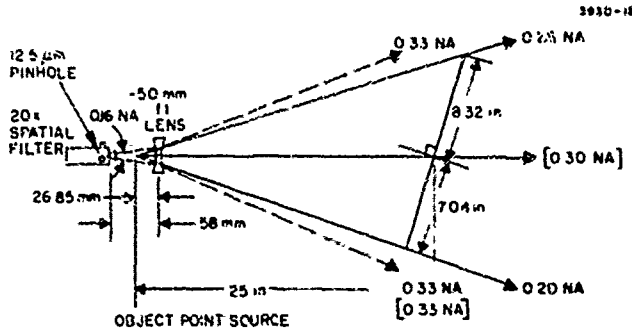


Fig. 3(a).  
Object beam numerical aperture requirement.

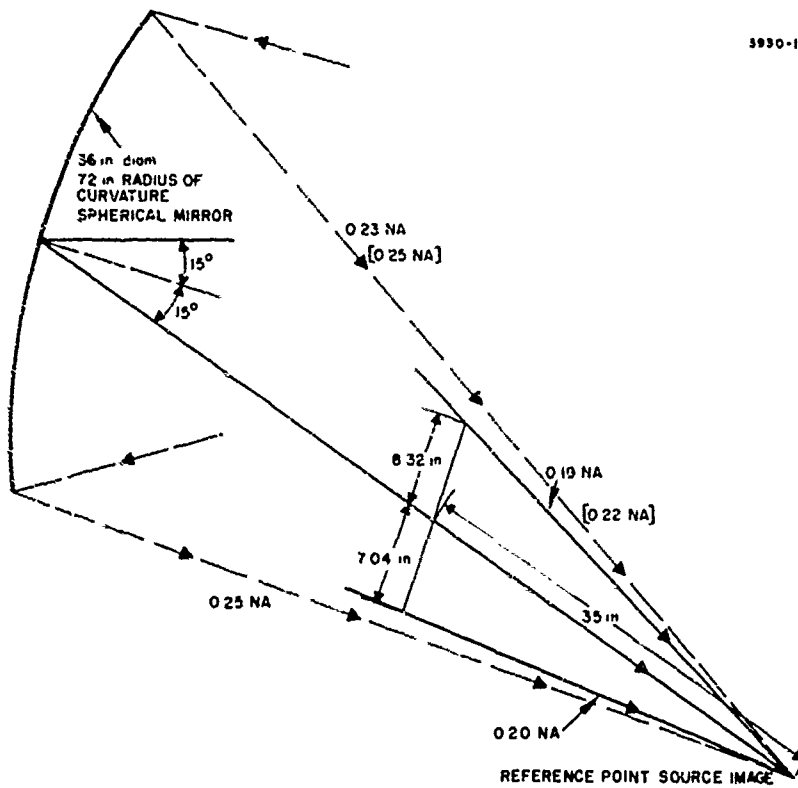


Fig. 3(b).  
Reference beam numerical aperture requirement.

## II. Construction Beam Optical System

### 3. REFERENCE BEAM CORRECTION OPTICAL SYSTEM

Two cylindrical lenses,  $\pm 8.170$  in. radius of curvature, located between the reference point source and the 72 in. radius of curvature mirror, provided optimum compensation of the tilted mirror aberrations to produce a reference image point blur diameter of less than 0.2 in. diameter.

The reference construction beam, as specified in Sections II-1 and II-2, was to converge from a 36 in. diameter, 72 in. radius of curvature spherical mirror to a point 35 in. behind the hologram. In order to provide proper clearance from the holographic plate holder, to meet the required size of the hologram aperture, and to minimize aberrations, the reference source and image points were located on lines  $\pm 15^\circ$  from the axis of the mirror. Correction optics, consisting of two cylindrical lenses,  $\pm 8.170$  in. radius of curvature, were computer-designed to provide optimum compensation of the large amount of astigmatism and coma in the reference image point due to the  $\pm 15^\circ$  off axis use of the spherical mirror. The resulting blur size of the corrected image point was reduced to less than 0.2 in., which meets the requirement for construction of the HUD hologram lens. The reference beam irradiance at the worst edge of the hologram aperture was less than 33% above the irradiance at the center of the hologram. This correction optics design and analysis was performed by Mr. John F. Belcher in the Optics Department of the Electro-Optical Division of Hughes Aircraft Company at Culver City, Los Angeles, California.

With the reference source and image point  $\pm 15^\circ$  from the optical axis of the 72 in. radius of curvature spherical mirror, the vertical (asymmetric) fan of rays of a reference point source 72 in. from the mirror focus to a horizontal line 67.37 in. away from the mirror, and the horizontal (symmetric) fan of rays focus to a vertical line 77.87 in. away from the mirror. This astigmatism, 10.5 in. separation between the two foci, is corrected by locating a pair of cylindrical lenses between the reference beam point source and the mirror, as shown in Fig. 4. This pair of  $\pm 8.170$  in. radius of curvature cylindrical lenses produces an apparent source 10.5 in. closer in the asymmetric direction than in the symmetric direction.

Tilting the negative cylindrical lens  $7^\circ$  in the asymmetric direction, as shown in Fig. 4, substantially reduces lower order coma, balancing the geometrical aberrations enough to reduce the blur diameter to less than 0.2 in. diameter. The resulting reference beam nonuniformity at the worst point was less than 33% above center illumination of the hologram.

The positive and negative cylindrical lenses were custom made at Harold Johnson Optical Laboratories in Los Angeles, California. Both cylindrical lenses were shaped out of fine annealed glass (Type 517-642) with a cylindrical surface quality of 1 fringe per in. The  $\pm 8.170$  in. radii of curvature of the positive and negative cylindrical lenses were held to a tolerance of  $\pm 0.05$  in. The cylindrical surfaces are coated for a reflectance of less than 0.5% at a wavelength of 647.1 nm.

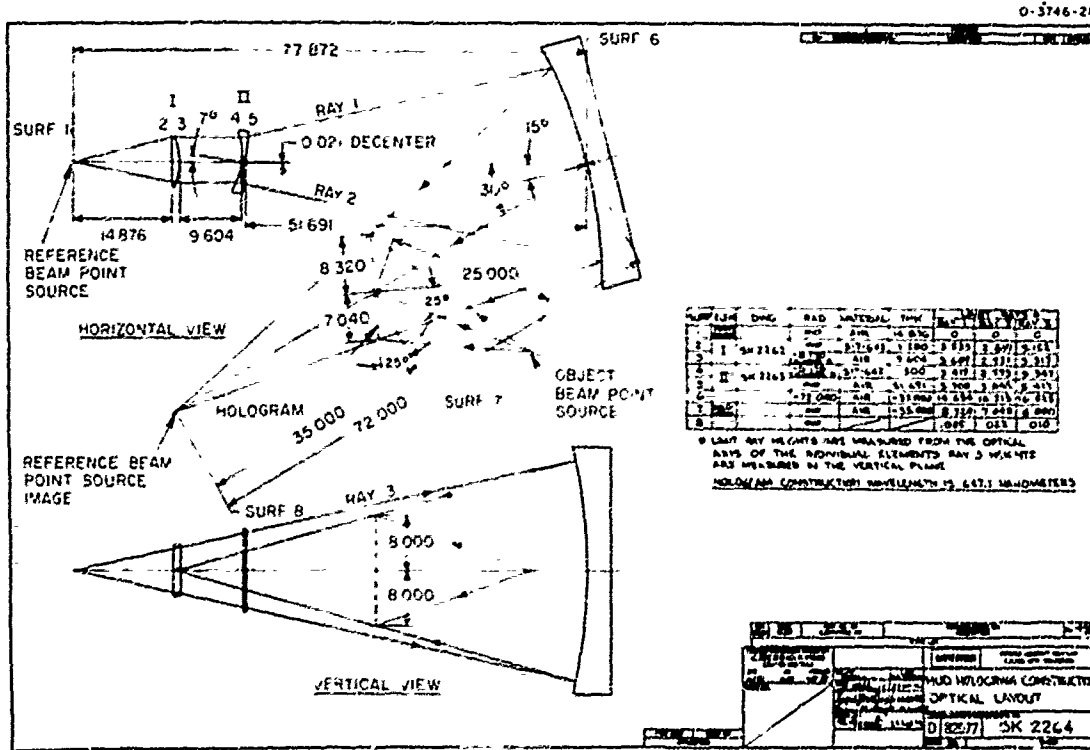


Fig. 4. HUD hologram construction beam optical layout with aberration correction cylindrical lenses in the reference beam.

## II. Construction Beam Optical System

### 4. CONSTRUCTION BEAM CHARACTERISTICS

Construction beams, consisting of an unaberrated object point source and a corrected reference point source image, in the recording apparatus exceed those required for construction of the full scale,  $50^\circ$  off-axis, symmetric transmission HUD lens.

The construction beam optical system of the full scale symmetric transmission hologram lens recording apparatus meets system specifications for a 3 in. high by 5 in. wide exit pupil with a 25 in. eye relief,  $25^\circ$  FOV, system  $f_0$  of 9 in., and the design requirement for high optical efficiency across the FOV at the center of the pupil. The construction beams consist of an unaberrated object point source at the center of the system exit pupil and a corrected reference point source image 35 in. behind the hologram. Aberrations in the reference point source image were reduced to a blur size of less than 0.2 in. to minimize angular deviation of the construction beam ray directions from the chief rays of the specified HUD system, thereby maintaining high chief ray efficiency. The remaining coma in the reference beam point source image can be taken into account along with the residual error of the HUD system during the relay lens design to reduce system errors to meet specifications.

The spatial filter/negative lens combination provides an object beam with uniform illumination across the hologram aperture. The characteristics of the corrected reference point source image from the spherical mirror are shown in Fig. 5(a). These show computer ray trace data for symmetric (x) and asymmetric (y) fans of rays, plotting intercepts at the reference point source image 35 in. behind the hologram versus the intercepts of the reference construction beam at the hologram aperture. The maximum deviation, shown on these geometrical aberration curves, of 0.1 in. from the location of an unaberrated point source image at the origin of the graph, corresponds to a  $2.86$  ( $\tan^{-1} 0.1/35$ ) mrad angular deviation from the chief ray of the system intercepting  $\pm 8$  in. of the symmetric hologram aperture. This angular deviation, compared to the angular half bandwidth deviation before diffraction efficiency drops to zero,  $\Delta\theta = n\lambda/t\sin\phi/2 = 192.22$  mrad,<sup>5</sup> will produce negligible loss of chief ray efficiency. In this equation the index of gelatin  $n = 1.54$ ,  $\lambda = 633$  nm, emulsion thickness  $t = 12$   $\mu\text{m}$ , and off axis angle  $\phi = 50^\circ$ . Figure 5(b) shows a photograph of the actual corrected reference beam point source image in the optical system. Near theoretically predicted reference beam point source imaging was obtained by the 36 in. diameter, 72 in. radius of curvature spherical mirror and computer designed correction optics.

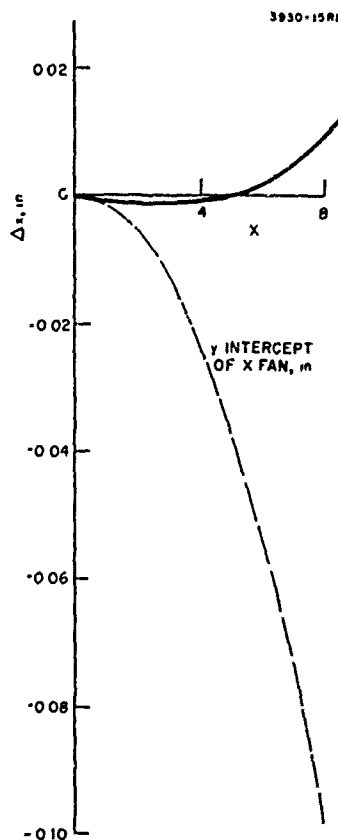
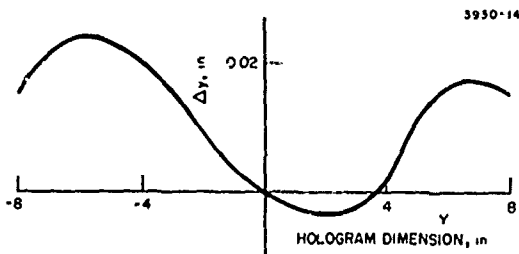


Fig. 5(a).  
Computer ray trace data of  
geometric aberration in  
the corrected reference  
point source image.

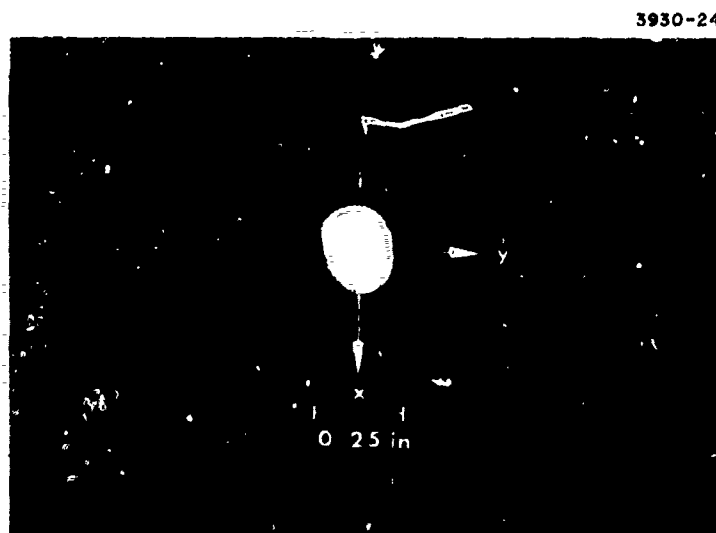


Fig. 5(b).  
Aberrations in the reference point source  
image were reduced to a blur size of less than  
0.2 in.

The construction beam irradiance illumination across the asymmetric hologram aperture shown in Fig. 6 was obtained starting with constant illumination from the reference point source. The gaussian illumination of a spatially filtered reference point source is used in the constructed recording apparatus to balance this illumination nonuniformity of the reference point source construction beam.

Reflection hologram lenses of the same geometry can also be recorded using this construction beam system. Depending on the particular design which specifies the construction geometry, additional wavefront shaping optics may be needed for a different off-axis angle usage of the large spherical mirror necessary to clear construction hardware.

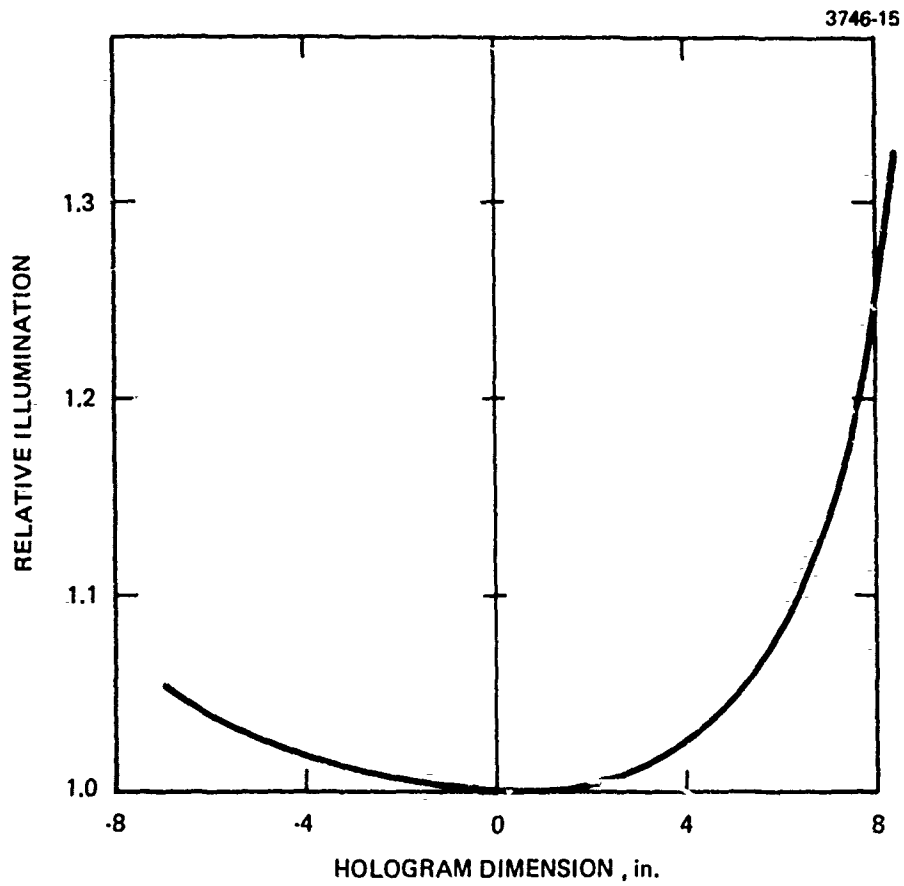


Fig. 6. Irradiance variation in the reference beam across the hologram aperture reduced to less than 33%.

### III. Environmental Isolation

#### 1. ENVIRONMENTAL ISOLATION REQUIREMENTS

Environmental isolation of the exposing apparatus from mechanical vibrations and airborne acoustic and thermal disturbances is required for fringe stability during the 1 to 2 hours (maximum) exposing period required for optimum efficiency using dye-sensitized dichromated gelatin.

The HUD continuous hologram lens is the recording of interference fringes between a spherical wavefront object beam and a spherical wavefront reference beam. High contrast fringes are ensured by careful path matching of the construction beam optical path lengths to the center of the hologram and keeping the illumination ratio of the beams near unity.

Stability of the interference pattern of the construction wavefronts at the light-sensitive emulsion during the time of exposure results in a high-contrast recording of the interference pattern. Instability due to building and mechanical vibrations, unstable optical components and airborne acoustic and thermal disturbances results in a time average recording of the interference pattern. Consequently, with instability there is a loss in recorded fringe contrast, index modulation  $\Delta n$ , and efficiency. Figure 7 depicts the recorded fringes for small bundles of rays from the construction beams. The recorded fringes lie parallel to the bisector of the included angle of the construction beams. For the  $50^\circ$  off-axis, symmetrical transmission recording configuration, the spacing between interference maximas is  $7.656 \times 10^{-7} \text{m} = \lambda/2n \sin \phi/2$ , which corresponds to a spatial frequency of 1306 cycles per mm. A shift of  $\lambda/2$  in relative phase of two construction beams will reverse the locations of fringe maxima and minima.

These interference fringes exist in space and are subject to motion of the holographic emulsion and substrate as well as environmental disturbance. However, for the transmission geometry where fringes lie perpendicular to the emulsion, fringe blurring due to motion in a direction perpendicular to the emulsion is not as critical as the same motion in reflection geometry where fringes lie parallel to the emulsion. This motion perpendicular to the emulsion is often observed in dichromated gelatin holographic emulsions, due to gelatin stress changes during exposure. Therefore, further optimization of the recording material and the plate mount may be required for successful development of large aperture reflection holograms.

We plan to use a commercial Krypton ion laser with 1 W output at 647.1 nm for recording the specified fullscale hologram. The path-length variation across the hologram aperture will require the use of an etalon to increase the coherence length of the laser, consequently

reducing the output power. Further power loss results from the exposing beams overfilling the hologram aperture to obtain uniform exposure across the large hologram aperture of approximately  $1300 \text{ cm}^2$ . The resulting low available exposing laser power per  $\text{cm}^2$  implies exposure times of up to 110 minutes. The large optical elements and construction hardware used to provide the construction beams and the long beam path lengths required to provide the proper construction geometry imply an unusual difficulty in attaining the high degree of long-term stability required in the exposure apparatus. Thus, environmental isolation by using low natural frequency supports for the optical table, stable construction hardware and acoustical shielding is required for high efficiency hologram lens construction.

3930-16

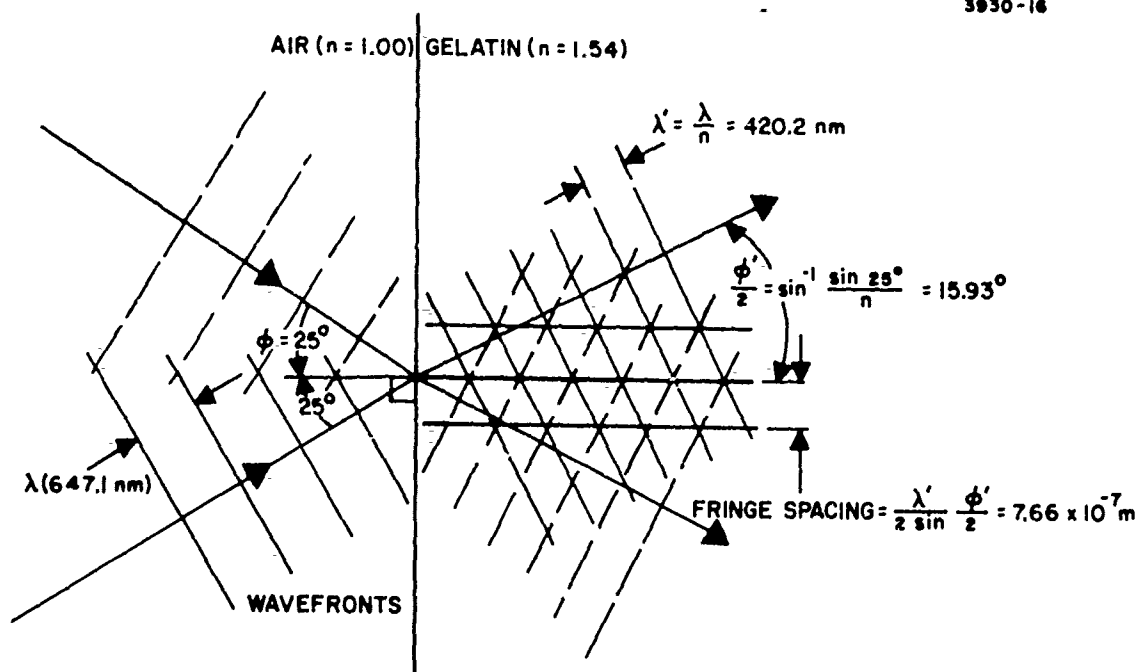


Fig. 7. Spatial frequency of 1306 fringe cycles per millimeter is recorded in  $50^\circ$  off-axis, transmission hologram.

### III. Environmental Isolation

#### 2. STRUCTURE-BORNE VIBRATION ISOLATION

A 5 ft x 10 ft x 10 in. thick granite optical table supported by six, low natural frequency pneumatic isolation mounts provides over 90% reduction of fringe instability arising from normal building vibrations.

A 5 ft x 10 ft x 10 in. thick granite optical table supported by six pneumatic isolation legs, procured from Newport Research Corporation, Fountain Valley, California, provides a vibration isolated surface on which the exposure apparatus is constructed. Granite has high thermal stability due to low conductivity coefficient ( $\lambda = 0.15$  Btu/in. -hr. - $^{\circ}$ F) and high specific heat coefficient ( $c = 19$  Btu/lb. - $^{\circ}$ F). The high mass density ( $\sim 200$  lb./ft $^3$ ) tends to act as an inertial block lowering the center of gravity of the recording apparatus.

The low resonance frequency ( $\sim 0.02$  Hz) of the six pneumatic, nitrogen-filled supports for the granite table, shown in Fig. 8, decouples the hologram recording apparatus from normal building vibrations due to in-building foot traffic, air conditioning systems, and other mechanical vibrations. Transmissibility of structure-borne vibrations is related to the frequency of the vibration and the resonance frequency of the vibration isolation support system,

$$T(\%) = \frac{100}{\left(\frac{f_d}{f_n}\right)^2 - 1}$$

These structure-borne vibrational frequencies,  $f_d$ , are typically much higher than the resonance frequency of the vibration isolation support system,  $f_n$ , resulting in low transmission of vibrational energy to the recording apparatus.

The bending modes and corresponding resonant frequencies of the 5 ft x 10 ft granite table top was measured at Newport Research Corporation by placing an accelerometer sensor at the center of the table top and driving the table with a 1-lb. force shaker at varying frequencies. Figure 9 shows a first order bending mode at 115 Hz and a torsional bending mode at 142 Hz. The low amplitude acceleration seen at the resonance frequency of 142 Hz shows the dynamic rigidity of granite. Small excitation at these structural resonant frequencies of the granite can result from airborne disturbances, but this excitation is effectively attenuated by the acoustical shield described in Section II-3 of this report. A high degree of structure-borne vibration isolation of the hologram recording apparatus on the granite optical table is verified in the performance evaluation (Section V) of the fringe stabilization system of the hologram recording system. Greater than 90% reduction in fringe motion due to structure-borne vibrations of 30 Hz was achieved by the vibration isolation system.

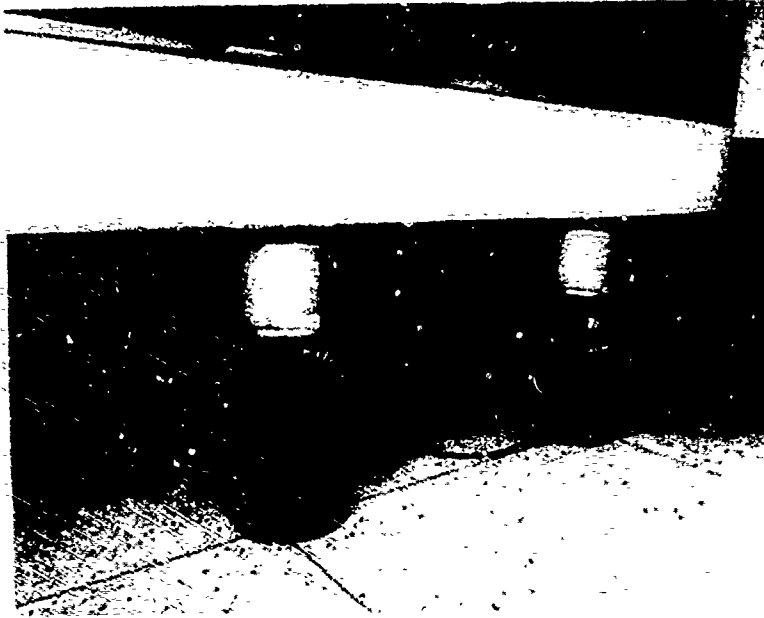


Fig. 8. Low resonance frequency ( $\sim 0.02$  Hz) pneumatic isolation mounts.

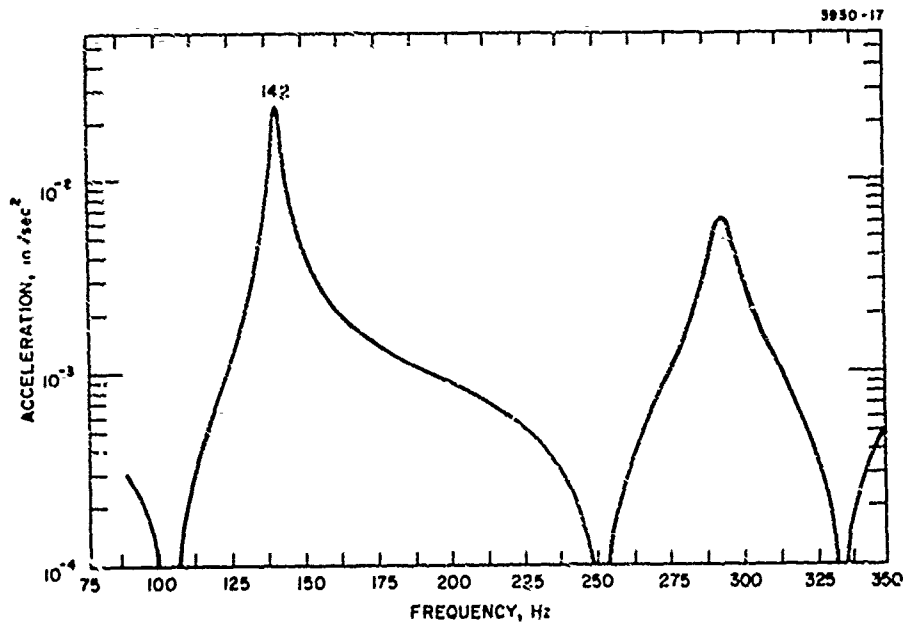


Fig. 9. First order bending mode at 115 Hz and torsional bending mode at 142 Hz at the center of the granite optical table due to one pound force.

### III. Environmental Isolation

#### 3. CONSTRUCTION HARDWARE - OPTICAL MOUNTS AND PLATE HOLDER

In-house design and construction of large-aperture optical mounts, vertical translators, and an 18 in. square plate holder provide stable mechanical mounting of the optical components on optical axes 19-1/4 in. above the granite table surface.

The 36 in. diameter spherical mirror required to form the proper construction beams for the HUD hologram lens sets the minimum height of the axes of the construction beams at 18 in. This height requirement, along with the large construction optics, set very high stability standards for the construction hardware, optical mounts, holographic plate holder, etc. Commercial optical mounts were used for the smaller aperture construction optics. However, there is no appropriate large optical hardware available on the market. Therefore, Mr. Cesar De Anda, Senior Research Associate with the Hologram Optics Section of Hughes Research Laboratories, did very careful construction hardware design work, relying on experience and iterative improvements during the construction and evaluation of the hologram recording apparatus. The primary design objective was for maximum stability. The resulting fringe stability of better than  $\lambda/20$  in the completed hologram recording apparatus (discussed in Section V) shows that the design objective was achieved.

To keep all beam heights as low as possible in the recording apparatus, the recording laser beam was separated into two levels. The lower level construction hardware and optics, consisting of small aperture plane mirrors, beam splitter, and a pzt translator, provides matching path lengths of 140 in. for each construction beam, measured from the beam splitter to the center of the hologram. The mounts for these components are magnetically mounted to steel plates bolted directly to the granite surface. The lower level beams from the beam splitter were then raised to the 19-1/4 in. height to obtain the two point sources required to form the construction beams. Figure 10 shows an example of the in-house construction hardware design consisting of 1-3/4 in. diameter, black-anodized aluminum posts, couplers and optical mounts. The vertical post, with two plane mirrors set at a  $45^\circ$  angle, is bolted directly to the granite. Optical mounts on the horizontal post, coupled to the vertical post, support the spatial filter and beam-expanding lens. Two other vertical posts give the entire assembly a stable, three-point support. This principle of interconnecting supports was also applied to the interferometer optical mount design shown in Fig. 11. Section IV, Fringe Control System, contains a detailed description of the interferometer design and application.

Optical mounts for the large spherical mirror and correction optics are shown in Figs. 12 and 13. The flat pyrex support on the back of the 36 in. diameter spherical mirror is bolted directly onto a vertical flat of the mount at three points, thus holding the mirror vertical with its

M10874



a

M10872



b

Fig. 10. Vertical translators with support posts provide stable mechanical mounting of construction optic.

optical center 19-1/4 in. above the granite table. The base of the mount is held down by L-joints bolted directly to the granite table. The frames containing the correction optics are supported by 1-3/4 in. posts magnetically mounted to a steel base bolted to the granite table.

Design and construction of the 18 in. square holographic plate holder, Fig. 11, was based on previous experience. Slots holding the holographic plate center 19-1/4 in. above the granite table allow the plate to reach a stable position without direct stresses being applied to the plate.

M10873

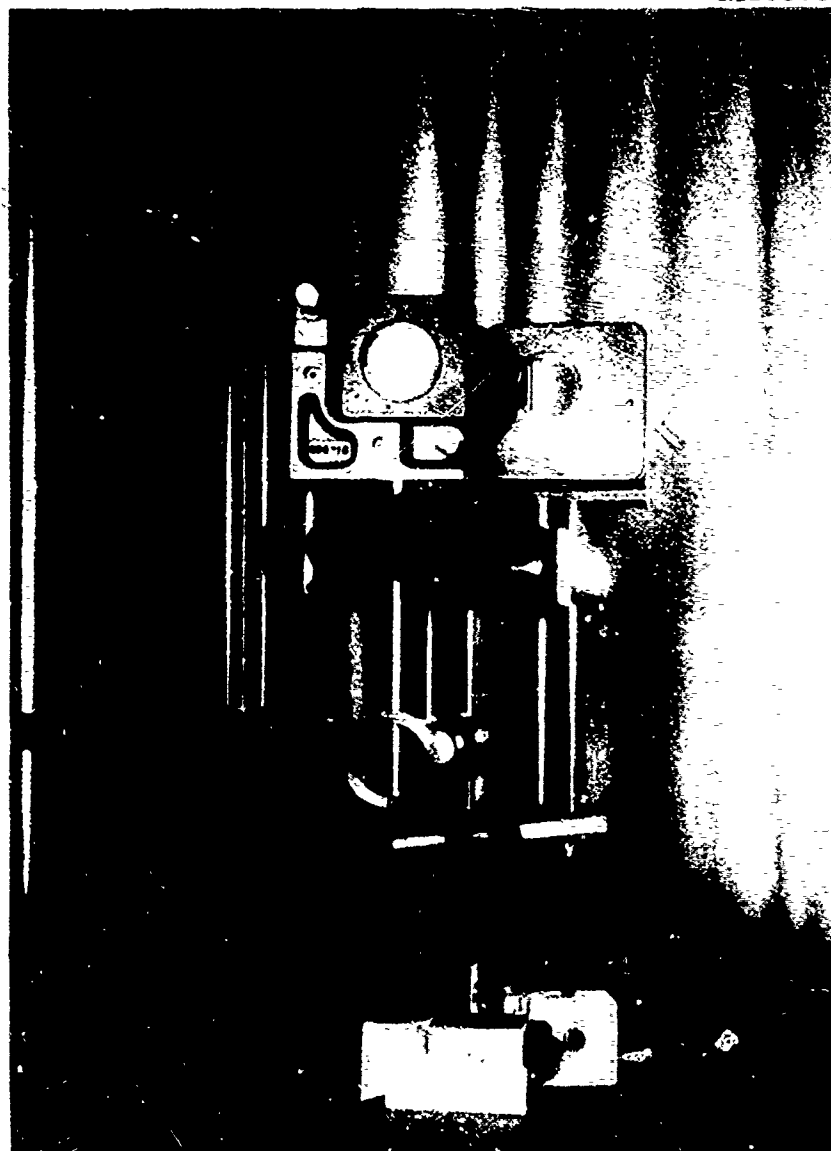


Fig. 11. Interferometer mount with interconnecting supports and 18 in. square holographic plate holder.

M10875

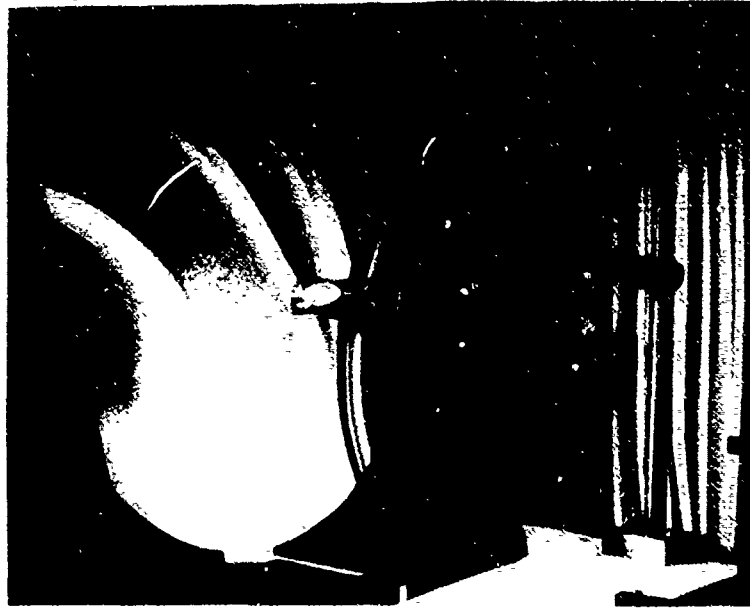


Fig. 12. Thirty-six in. diameter, 72 in. radius of curvature spherical mirror is mounted vertically.

M10871



Fig. 13. Cylindrical correction element mounts.

### III. Environmental Isolation

#### 4. AIR-BORNE VIBRATION ISOLATION

A 5 ft x 9 ft x 40 in. high acoustic enclosure, consisting of 6 lb./ft<sup>3</sup> mineral wool sandwiched between 24 gauge sheet steel and 26 gauge perforated sheet steel provides high transmission loss for acoustical noise, air turbulence, and other air-borne disturbances.

A 5 ft x 9 ft x 40 in. high acoustic enclosure attenuates acoustic noise at the resonance frequencies of various bending modes of the granite surface and construction hardware, and shields the hologram construction apparatus from thermal gradients and air turbulence. The 2 in. thick acoustic enclosure consists of 6 lb./ft<sup>3</sup> density of mineral wool sandwiched between an inner, 26-gauge, perforated steel panel and an outer, 24-gauge, steel panel. A close-meshed, flat black cloth between the mineral wool and inner panel prevents loose material from falling on the construction optics and minimizes stray reflection of the construction beams. Six removable panels allow quick access to construction optics and the holographic plate holder. Figure 14 is a cross-sectional material sketch of the acoustic enclosure.

The acoustic enclosure, manufactured at Webster Product Co., Anaheim, California, utilizes both dense and porous materials in a double-wall construction to provide high transmission loss and damping of environmental air-borne disturbances. The outer 24-gauge steel with a surface density of ~40 lb./ft<sup>2</sup> per in. thick, highly restricts the passage of sound and air turbulence. It has high transmission loss, low acoustic absorption, and high reverberation. The 6 lb./ft<sup>3</sup> mineral wool, a fibrous material, absorbs transmitted sound with little reverberation. High acoustic frequencies, >100 Hz, are attenuated due to friction loss of acoustically generated air motion through the pores of the mineral wool. The perforated 26-gauge inner panel permits further absorption of transmitted acoustical noise with minimum reverberation in the enclosure.

High attenuation of frequencies >100 Hz was evaluated and discussed in detail in the performance evaluation, Section V, of this report. Acoustical perturbation at the resonant frequencies of the bending modes of the granite at 115 Hz and 140 Hz were effectively damped by the enclosure.

3746-18

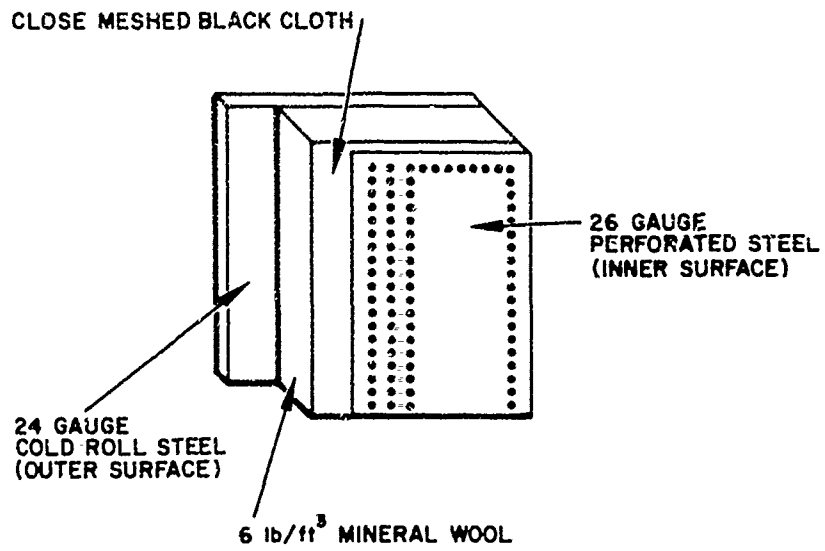


Fig. 14. Cross-section material sketch of acoustic enclosure.

#### IV. Fringe Control System

##### 1. INTERFERENCE FRINGE STABILITY REQUIREMENTS

Maximum-efficiency recording of the HUD hologram lens requires relative phase stability of the two construction point source beams at the hologram recording plane.

The construction of the HUD hologram lens requires recording stationary amplitude and phase information in the interference field formed by the combination of the specified construction beams at the hologram recording plane. The intensity,  $I = K[A_0^2 + A_r^2 + 2A_0A_r \cos(\psi_0 - \psi_r)]$ , of the interference pattern at each point on the hologram recording plane is a function of amplitudes  $A_0$  and  $A_r$  and the phase difference,  $\psi_0 - \psi_r$ , of the construction waves of the object and reference beams at that point. There is maximum intensity at points where the phase difference is an even multiple of  $\pi$  and minimum intensity where the phase difference is an odd multiple of  $\pi$ . Maximum interference fringe contrast results if the amplitudes of the construction beams are equal and the coherence length of the laser source is not exceeded.

During an exposure of time  $\tau$ , the relative phase differences are subjected to variations, due to mechanical and acoustical perturbations and thermal changes of optical elements and mounts. These perturbations change the effective path length difference of the construction waves which is related to the phase difference by  $2\pi(S_0 - S_r)/\lambda = (\psi_0 - \psi_r)$ . Constant phase difference during an exposure  $\tau$  implies high contrast standing interference fringes in space at the hologram recording plane. A stable holographic plate will record the instantaneous intensities of the interference fringes, defined by eq. (3) which contains both amplitude and phase information of the interfering wavefronts. The resulting HUD hologram lens has maximum efficiency as a result of this high-contrast recording of stable interference fringes.

Phase perturbations during the exposure  $\tau$  degrade recording fringe contrast caused by fringe instability, resulting in a time average intensity recording of interference fringes. If the relative phase difference changes by  $\pi$ , linearly over the exposure period  $\tau$ , all phase information is lost during the exposure, resulting in a uniform intensity recording or zero diffraction efficiency. This is shown mathematically in Fig. 15, where eq. (6) shows that the resultant time average exposure at every point in the hologram recording plane becomes dependent only on the amplitudes of the construction beams.

A perturbation causing a relative path length change of  $\lambda/2$  during the exposure period, where  $\lambda$  is the recording laser wavelength, can cause a relative phase change of  $\pi$  at the hologram recording plane. With a 632.8 nm He-Ne laser,  $\lambda/2$  is equal to 316.4 nm. Although good mechanical stability and environmental isolation was achieved in the

full scale recording apparatus, thermal changes in optical elements and mounts can cause the wavefronts of the construction beams to shift relatively by  $\lambda/2$ , consequently shifting the phase difference at every point in the interference field at the hologram recording plane by  $\pi$ . In this section we discuss the design, analysis, and construction of a fringe control system, consisting of an interferometer phase detection system and feedback electronics, along with photodetectors and a PZT mirror translator. Relative phase or path length variation of the construction beams during exposure is detected and corrected to reduce  $\delta\psi(t)$  to an acceptable level for high efficiency HUD hologram lens recording.

$$I(t) = K[A_0^2 + A_R^2 + 2A_0A_R \cos([\phi_0 - \phi_R] + (\phi_0(t) - \phi_R(t)))] \quad \text{Equation 1}$$

$I(t)$  = interference intensity of the reference and object construction beams

$A_0$  = amplitude of the object construction beam

$A_R$  = amplitude of the reference construction beam

$[\phi_0 - \phi_R]$  = relative phase of the construction wavefronts at the hologram recording plane

$[\phi_0(t) - \phi_R(t)]$  = relative phase perturbation of  $[\phi_0 - \phi_R]$

$K$  = proportionality constant

$$\text{Exposure } E = \int_0^L I(t) dt \quad \text{where } L = \text{length of exposure} \quad \text{Equation 2}$$

For stable interference fringe:

$$\begin{aligned} \phi_0(t) - \phi_R(t) &= 0 \\ E &= \int_0^L K[A_0^2 + A_R^2 + 2A_0A_R \cos(\phi_0 - \phi_R)] dt \\ &= K[A_0^2 + A_R^2 + 2A_0A_R \cos(\phi_0 - \phi_R)] \end{aligned} \quad \text{Equation 3}$$

For unstable interference fringe:

If  $\phi(t) = t/L$  linear phase perturbation of  $\phi$  over the exposure length

$$E = \int_0^L K[A_0^2 + A_R^2 + 2A_0A_R \cos([\phi_0 - \phi_R] + t/L)] dt \quad \text{Equation 4}$$

$$\begin{aligned} &= K[A_0^2 + A_R^2 + 2A_0A_R \int_0^L \cos([\phi_0 - \phi_R] + t/L) dt] \\ &\quad + \sin([\phi_0 - \phi_R] + t/L) \Big|_0^L \end{aligned} \quad \text{Equation 5}$$

$$= K[A_0^2 + A_R^2] \quad \text{Total loss of phase information} \quad \text{Equation 6}$$

Fig. 15. Phase perturbation during exposure of a hologram causes reduction of recorded fringe contrast.

#### IV. Fringe Control System

##### 2. INTERFEROMETER PHASE DETECTION SYSTEM

The interferometer system reduces the angle between the construction beams behind the hologram recording plane, providing low spatial frequency fringes for efficient detection of relative phase between the object and reference construction beam wavefronts.

The spacing between fringe maximas in the area near the center of the hologram aperture is equal to  $d = \lambda/2n\sin\theta/2$ , where the recording wavelength  $\lambda = 632.8$  nm, the index of refraction of gelatin  $n = 1.54$  and the included angle between construction beams in gelatin  $\theta = 31.86^\circ$ . This spacing of  $7.487 \times 10^{-7}$  m corresponds to a spatial frequency of 1335.71 cycles per mm. To detect sinusoidal phase dependent intensity variations, the detection system would have to resolve a width much less than  $7.487 \times 10^{-7}$  mm.

The interferometer system, as shown in Fig. 16, was constructed using plane mirrors, a beam splitter, and wavefront-shaping optics in the diverging object beam. The configuration provides matched path lengths from the center of the hologram recording plane to the point of interference where the beam splitter combines the object and reference beams to form low spatial frequency interference fringes for easy detection. Two identical,  $180^\circ$  out of phase, low spatial frequency interference patterns are formed on opposite sides of the beamsplitter as a result of a  $\pi/2$  phase shift experienced by wavefronts reflecting off the beam splitter. The intensity resulting from the interference of any two interferometer waves can be expressed as

$$I_i = K \left[ A_{O_i}^2 + A_{R_i}^2 + 2A_{O_i} A_{R_i} \right] \cos \left[ \left( \phi_{O_i}(t) - \phi_{R_i}(t) \right) - \left( \alpha_{O_i} - \alpha_{R_i} \right) \right].$$

The mathematical derivation is shown in Fig. 16. The wave shaping optics change the effective path length difference of each combining ray such that

$$\left( \phi_{O_i}(t) - \phi_{R_i}(t) \right) - \left( \alpha_{O_i} - \alpha_{R_i} \right)$$

is constant at every point in the interference resulting in a single fringe of uniform intensity.

The initial phase at the hologram recording plane,  $\phi_{O_i}(t)$  and  $\phi_{R_i}(t)$ , are also subject to perturbation due to relative path length difference variations of the construction beams with respect to time. Only perturbations uniform over the aperture of the construction beam shall be considered. The detection and correction of nonuniform perturbations is not feasible

$$v_{o_i} = A_{o_i} e^{j(\phi_{o_i}(t) - \phi_{o_i})} \quad v_{R_i} = A_{R_i} e^{j(\phi_{R_i}(t) - \phi_{R_i} + \pi/2)}$$

$v_{o_i}$  &  $v_{R_i}$  = complex amplitude of interfering object and reflected reference wave after the beam splitter at the detector

$\phi_{o_i}(t)$  &  $\phi_{R_i}(t)$  = initial phase of object and reference wave at the hologram recording plane

$\phi_{o_i}$  &  $\phi_{R_i}$  = phase of the object and reference wave at the detector

$\pi/2$  = beamsplitter phase shift on reflected reference wave

$\phi_i$  = combined wave motion of object and reference wave at the detector

$$= (\phi_{o_i} + \phi_{R_i})$$

$I_i$  = intensity of the combined wave motion at the detector

=  $K[\phi_i^2]$  where K is a proportionality constant

$$= K[A_{o_i}^2 + A_{R_i}^2 + 2A_{o_i}A_{R_i} \cos [(\phi_{o_i}(t) - \phi_{R_i}(t)) - (\phi_{o_i} - \phi_{R_i}) - \pi/2]$$

$I$  = total intensity of the interference of all reference and object wave on the detector

$$= \sum_{i=1}^n I_i \quad \text{where } n \text{ is the number of interfering waves}$$

Perfect overlap of all interfering waves =  $[(\phi_{o_i} - \phi_{R_i}) - (\phi_{o_i} - \phi_{R_i})] = \text{constant}$

for all  $i$  in the absence of phase perturbation  $\therefore$  interference intensity on the detector is uniform, i.e., forms one fringe.

Linear phase perturbation on all intersecting wavefronts at the hologram recording plane =  $(\phi_{o_i}(t) - \phi_{R_i}(t)) = \text{constant for all } i$ .

$$\text{Therefore: } I = K[A_o^2 + A_R^2 + 2A_oA_R \cos (\phi_o(t) - \phi_R(t) - \pi/2)$$

where  $A_o$  &  $A_R$  = amplitudes of intersecting axial wavefronts at the center of the hologram

$\phi_o(t)$  &  $\phi_R(t)$  = axial phase of the object and reference construction beam at the center of the hologram.

Note: The resultant interference intensity due to the transmitted reference wavefront and reflected object wavefront on the opposite side of the interferometer beam splitter is:

$$I = K[A_o^2 + A_R^2 + 2A_oA_R \cos (\phi_o(t) - \phi_R(t) + \pi/2)$$

Fig. 16. Interferometer system expands the relative axial fringe at the hologram recording plane for high efficiency detections of axial phase instability of the construction beams.

due to the need to detect and correct the relative phase difference of each individual area of the hologram construction wavefronts. These nonuniform perturbations generally are associated with airborne turbulence and vibration which is eliminated by environmental shielding. Uniform perturbations, from thermal expansion of optical elements and mounts during long exposures, uniformly perturb the entire area of the construction beams at the hologram recording plane, so that every interference fringe suffers the same variation in intensity due to the same relative phase perturbation. We make the additional assumption that there is no additional wavefront perturbation added in the interferometer system. The optical elements in the interferometer are small and closely-spaced, compared to the construction optics used to meet the construction beam specifications, and mechanical mount design provides the necessary stability required to hold the optical axis of the interferometer system at the height of the construction beams optical axis.

Based on these assumptions, the uniform variation of intensity of the interferometer fringe pattern, corresponding to a phase perturbation of the construction beam wavefronts passing through the 1 in. diameter area of the hologram recording plane, defines the phase difference between these wavefronts. Mathematically,

$$I = K \left( A_o^2 + A_r^2 + 2A_o A_r \right) \cos \left( \phi_o(t) - \phi_r(t) \right) ,$$

where  $A_o$  and  $A_r$  are the amplitudes of the wavefronts, and  $(\phi_o(t) - \phi_r(t))$  is the axial phase difference between the two construction beams at the hologram recording plane. The interferometer essentially expands the axial fringe of the high spatial frequency interference pattern at the hologram recording plane, forming a single fringe which fills the interferometer aperture for efficient detection.

A slight mismatch between the interferometer wavefronts in the actual system, due to residual aberrations in the reference point source image, causes more than one fringe to be formed in the interference pattern, as shown in Fig. 17. The central fringe in the interference pattern contains enough intensity and is large enough for easy detection of phase instability in the construction wavefronts. A change from maximum to minimum intensity in the fringe intensity corresponds to a phase difference change of  $\pi$  or a relative path length difference change of  $\lambda/2$  between the construction wavefronts at the hologram plane.

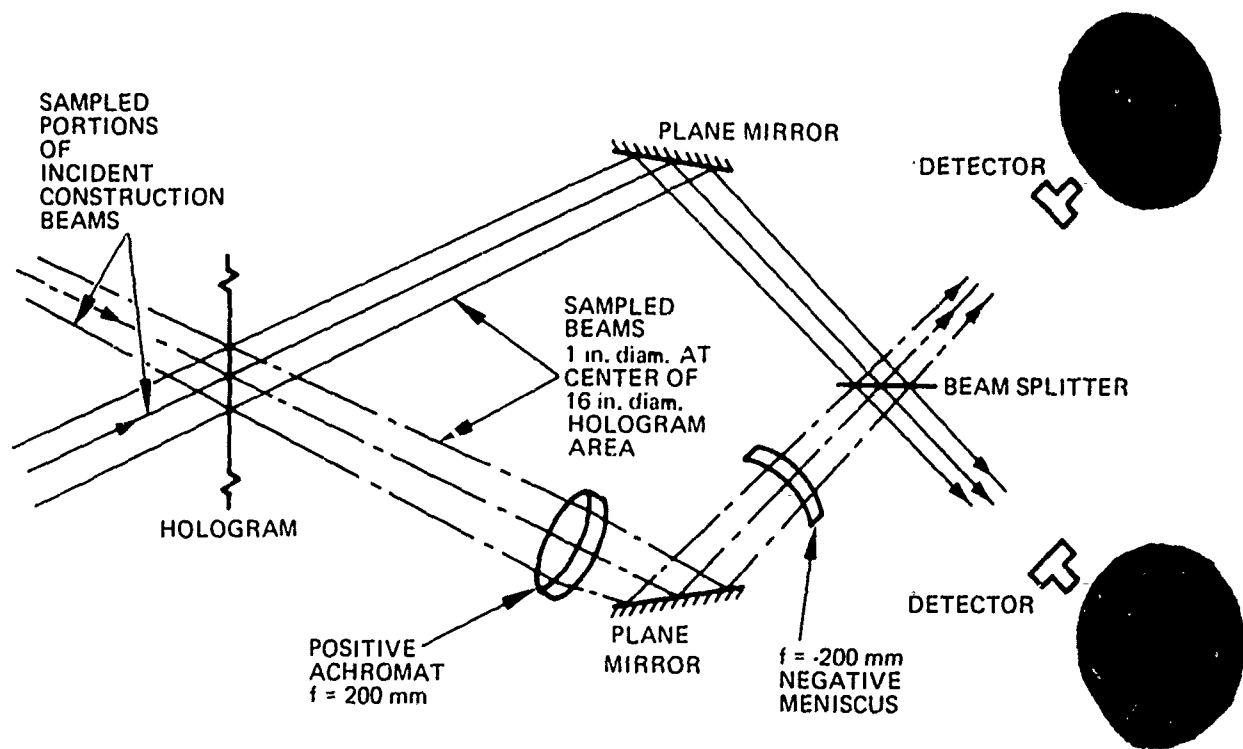


Fig. 17. Two identical,  $180^\circ$  out of phase, low spatial frequency interference patterns are formed.

#### IV. Fringe Control System

##### 3. WAVEFRONT SHAPING OPTICS REQUIREMENT

A 40 mm diameter, 200 mm focal length achromat and a 55 mm diameter, -200 mm focal length, meniscus lens reshape the wavefront of the diverging object beam to match the aperture and convergence of the reference beam.

The wave-shaping optical system in the interferometer shapes the diverging object beam so that each ray of the object beam, within a 1 in. diameter area of the hologram aperture center, can be made to overlap with the corresponding ray from the converging reference beam. The 1:1 construction beam intensity ratio at the hologram recording plane is preserved in the interferometer beams because of the one-to-one mapping of intersecting wavefronts of equal intensity. This implies low spatial frequency radial interference fringes with maximum fringe contrast.

The optical system of the interferometer must converge the diverging object beam to a point source image 35 in. behind the hologram with the same numerical aperture as that of the converging reference beam transmitted through the same area. Two waveshaping elements were used, as shown in Fig. 18. The positive element first converges the diverging beam while the negative element provides the proper length and numerical aperture. Any set of optical elements satisfying the systems equations can be used. Based on these equations, interferometer layout constraints, and optical element size and availability, a 40 mm diameter positive achromat lens with a focal length of 200 mm and a 55 mm diameter negative meniscus lens with a focal length of -200 mm were chosen. Figure 19 shows locations of these waveshaping optics with reference to distances along the optical axis to other elements in the interferometer system. The slight mismatch from perfect mapping has little effect on the spatial frequency, interference fringe contrast, and performance of the interferometer system.

This basic interferometer design can be applied to any hologram lens construction geometry, both reflection and transmission configurations. The limiting factor in applying this interferometer design to other construction geometries and configurations would be possible obstruction of the construction beams due to limited working area on the 5 ft x 10 ft granite surface. Different wave-shaping optics may be required to obtain proper mapping of the construction beams depending on the construction beam geometry.

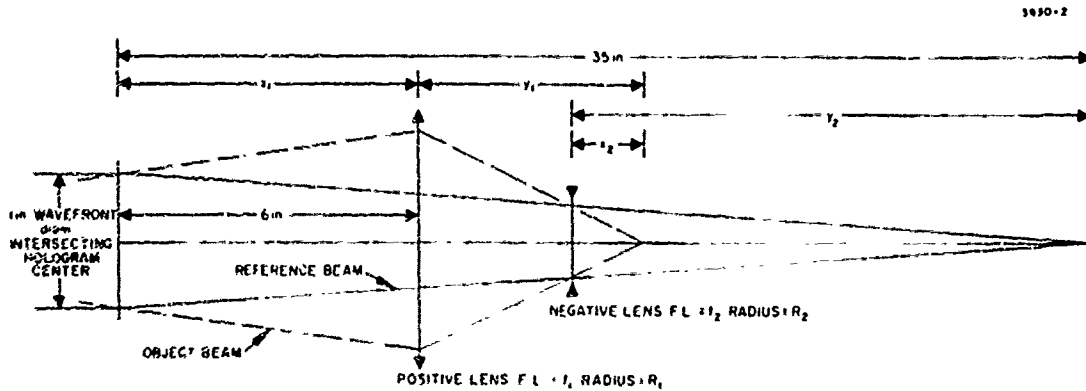


Fig. 18. A 200 mm f. l. positive achromat converges the diverging object beam, and a -200 mm f. l. negative meniscus provides the proper length and numerical aperture.

SYSTEM EQUATIONS:

$$\frac{1}{25 + X_1} + \frac{1}{Y_1} = \frac{1}{f_1} \quad \Rightarrow \quad Y_1 = 10.55 \text{ in.}$$

$$\frac{0.5}{25} = \frac{R_1}{25 + X_1} \quad \Rightarrow \quad R_1 = 0.62 \text{ in.}$$

$$X_2 \left( \frac{R_1}{Y_1} \right) = \frac{0.5}{35} \left( X_2 + [35 - X_1 - Y_1] \right) \quad \Rightarrow \quad X_2 = 5.93 \text{ in.}$$

$$R_2 = X_2 \frac{R_1}{Y_1} \quad \Rightarrow \quad R_2 = 0.35 \text{ in.}$$

$$\frac{1}{-X_2} + \frac{1}{(35 - X_1 - Y_1 + X_2)} = \frac{1}{f_2} \quad \Rightarrow \quad f_2 = -199.03 \text{ mm}$$

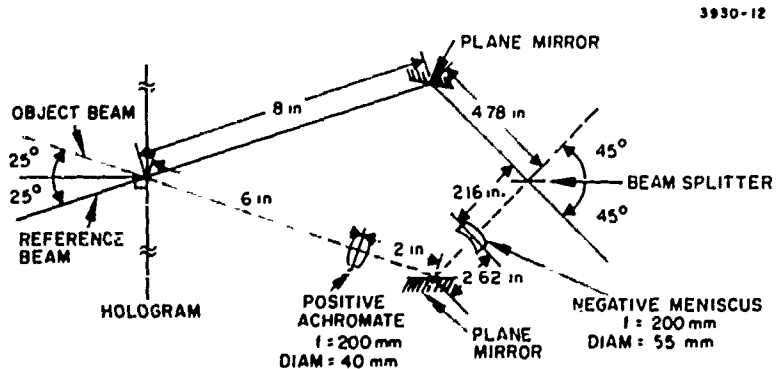


Fig. 19. Optical layout of the interferometer system.

#### IV. Fringe Control System

##### 4. FRINGE CONTROL ELECTRONICS SYSTEM

The interference fringes of the object and reference construction beams at the hologram recording plane are stabilized in space by feedback electronics<sup>6</sup> which actively control the phase of the object beam wavefronts by translating a plane mirror until the balanced output of the interferometer fringe detectors are equal.

The interferometer fringe amplitudes measured by the detectors are

$$I_A = K \left( A_o^2 + A_r^2 + 2A_o A_r \right) \cos \left( \phi_o(t) - \phi_r(t) + \frac{\pi}{2} \right)$$

and

$$I_B = K \left( A_o^2 + A_r^2 + 2A_o A_r \right) \cos \left( \phi_o(t) - \phi_r(t) - \frac{\pi}{2} \right)$$

where  $A_o$  and  $A_r$  are the amplitudes of the construction beams at the hologram plane, and  $\phi_o(t) - \phi_r(t)$  is the phase difference. By stabilizing phase difference, the fringes at the hologram recording plane are stabilized in space.

The use of two detectors and an interferometer design which provides two fringes  $\pm \pi/2$  out of phase provides a balanced output that is insensitive to laser power level changes during the long exposure. This difference output,  $I_A - I_B$ , equals  $-4K A_o A_r \sin \left( \phi_o(t) - \phi_r(t) \right)$ . Not only is the sensitivity of the detection signal increased due to an increase in the amplitude of the sinusoidal intensity variation, but a change in laser power level is not seen by the control electronics if the phase difference is locked at a value of zero. This also locks the phase difference at a value where small  $\phi_o(t) - \phi_r(t)$  variations are detected with maximum sensitivity.

The feedback fringe control electronic system constructed for the full-scale HUD hologram recording apparatus is shown in the block diagram in Fig. 20. Silicon photodiodes, with a response of 0.26 to 0.27  $\mu\text{A}/\mu\text{W}$ , convert the fringe intensities to proportional electrical currents. The high-gain, current-to-voltage amplifiers present a low impedance to the detectors, converting very low level currents to voltages approximately equal to the input current times the feedback resistor. Five values of gain were incorporated in the amplifier to maximize the output voltage swing corresponding to a maximum-to-minimum fringe intensity change seen by the detectors. High signal-to-noise detection was obtained by the use of chopper-stabilized amplifiers, careful shielding of wiring, and unbiased silicon photodetectors.

The difference integrator has a rise time of 1 sec. Any phase perturbation causes an increase in intensity at one detector and a corresponding decrease in the other, creating an error signal into the integrator. The integrator output is amplified by a high voltage amplifier and used to drive a PZT translator. The amplifier effectively increases the dynamic range of the integrator, since a PZT translating a plane mirror (1.15  $\mu\text{m}$  per 100 V) in the object construction beam leg can track and correct through several fringe cycles before the integrator's  $\pm 10$  V saturation is reached. This translation changes the relative phase, driving it back to zero, and stabilizing the fringe pattern at the holographic plate.

Precautions must be taken to allow the holographic plate to stabilize in order to record the stable interference fringe. Although plate motion in the direction normal to the holographic plate surface does not blur the recorded fringes which are also normal to the surface in symmetric transmission holograms, any plate motion may cause erroneous path length shifts in the interferometer, resulting in an erroneous phase correction. However, with sufficient holographic plate stabilizing time, the holographic plate will record high contrast fringes, resulting in a high efficiency, large aperture, HUD hologram lens.

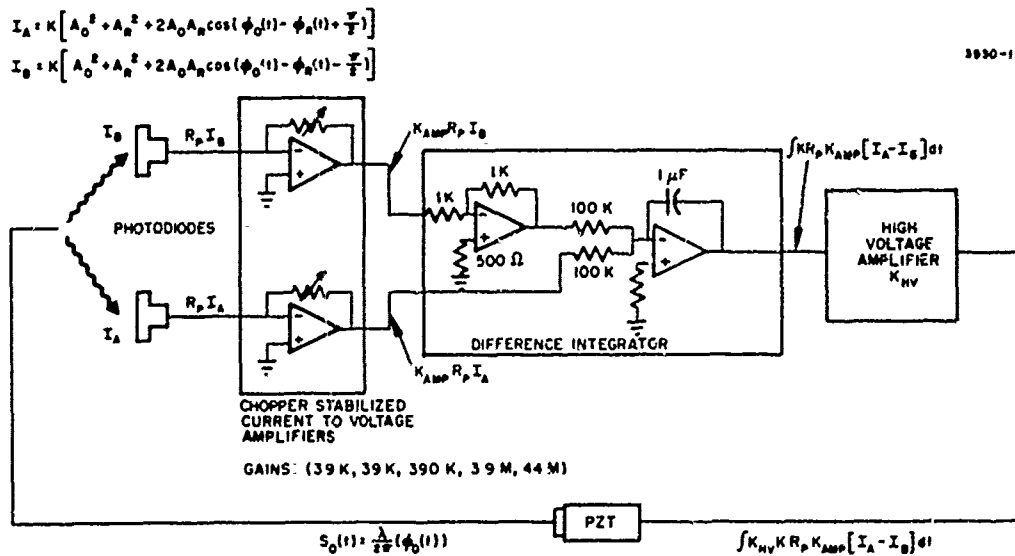


Fig. 20. Feedback electronic corrects axial phase instability by translating a plane mirror in the object beam.

- $R_p$  = detector response  $\sim 0.26 \mu\text{A}/\mu\text{W}$
- $K_{amp}$  = amplifier gain
- $K_{HV}$  = high voltage gain
- $s_o(t)$  = path length correction

## V. Performance

### 1. FULL-SCALE HOLOGRAM LENS RECORDING SYSTEM

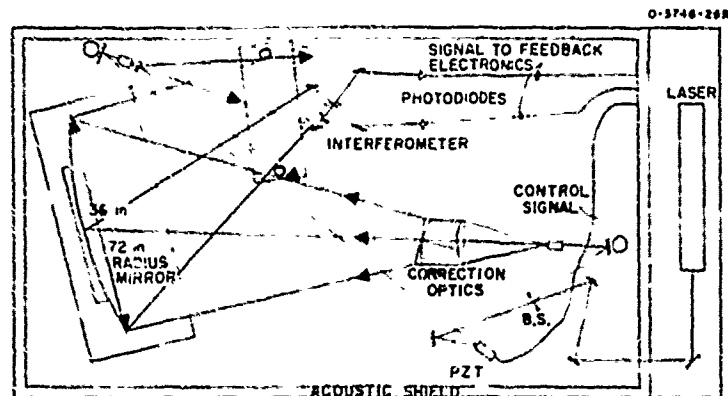
The full-scale hologram lens recording system consists of construction optics assembled to provide the specified construction beams for a  $50^\circ$  off-axis, symmetric transmission hologram, granite table with pneumatic supports, acoustical shield and a feedback fringe control system.

The recording apparatus layout, shown in Fig. 21, was constructed for recording  $50^\circ$  off-axis, symmetric transmission holographic HUD lenses which meet the NADC system specifications for a circular  $25^\circ$  FOV in an exit pupil 3 in. high by 5 in. wide with a 25 in. eye relief. The recording apparatus layout provides the proper construction wavefronts with plane mirrors, beamsplitters, spatial filters, a 36 in. diameter 72 in. radius of curvature spherical mirror along with cylindrical correction elements while providing clearance from construction hardware. The recording apparatus is enclosed with a 5 ft x 9 ft by 40 in. high acoustic shield on a 5 ft x 10 ft x 10 in. thick granite optical table supported by six pneumatic isolation supports. The laser source on the optical table provides the laser beam through a small aperture in the acoustic shield where the transmitted object beam and reflected reference beam originate at the beam splitter. The axial optical path length of each construction beam is 140 in. from the beamsplitter to the center of the hologram, 19-1/4 in. above the granite surface. The resultant path length difference at the extremes of the hologram aperture, +8.32 in. and -7.04 in. from the center, is 17 cm. The axial object and reference beams intersect at the center of the required hologram aperture in the hologram recording plane with a  $50^\circ$  included angle. The normal to the hologram recording plane containing the 18 in. square holographic plate holder bisects the  $50^\circ$  included angle, thereby forming a symmetric transmission hologram with a  $50^\circ$  off-axis angle.

The object beam, transmitted by the beamsplitter is directed, with a plane mirror mounted on a piezoelectric translator, toward a beam steering unit which raises the beam height up to 19-1/4 in. above the granite surface, where a 20X spatial filter/-50 mm focal length lens assembly forms an object point source 25 in. from the hologram center. The reference beam, reflected by the beamsplitter, is also raised up to a 19-1/4 in. height, where a 40X spatial filter forms a reference point source 77.872 in. from the spherical mirror reflecting at  $30^\circ$  angle. Aberrations in the reflected reference point source image, 35 in. behind the center of the hologram, are reduced to an acceptable level by two cylindrical correction elements. The resultant  $50^\circ$  off-axis, symmetric transmission hologram lens has a focal length of 14.58 in.

The phase detecting interferometer and silicon photodetectors interrogates the axial phase difference of the construction beams. A control signal from the feedback electronics to the piezoelectric translator controls the phase of the object beam by translating a plane mirror. The closed-loop system locks the relative axial phase of the object and reference construction beam to provide fringe stability across the hologram aperture.

Fringe stability evaluations were made using the interferometer phase detection system to detect relative phase difference of the axial phase. A 632.8 nm HeNe laser was used to evaluate the isolation performance of the granite table with pneumatic support and acoustic shield. The performance of the fringe control system was also evaluated, and a high degree of fringe stability over long periods was achieved, with enough dynamic range to extend fringe control for several hours.



M10870



Fig. 21. Full-scale, 50° off-axis, symmetric transmission hologram lens recording system.

V. Performance

2. ENVIRONMENTAL ISOLATION - SHORT TERM FRINGE STABILITY

Environmental isolation and stable construction hardware attenuates fringe instability due to mechanical and airborne vibrations, but long term fringe instability can be caused by thermal changes in optical elements and mounts.

The fringe stability of the assembled full-scale hologram recording apparatus was evaluated using the interferometer phase detector. The full fringe depth calibration, a change from maximum to minimum interference intensity, corresponds to a  $\pi$  phase shift in the phase difference between construction wavefronts at the hologram recording plane, i. e., a  $\lambda/2$  relative path length shift. The calibration of a full fringe depth is shown in Fig. 22, which shows the amplified output of one of the photodetectors as the piezoelectric translator is used to induce a path length change between the construction beams.

The performance of the pneumatic supported 5 ft x 10 ft granite optical table can be seen in Fig. 23. Without the pneumatic support, the fringe instability due to normal building vibration of approximately 30 Hz is 59% of a full fringe depth. This fringe instability would cause dramatic efficiency loss in recorded efficiency even for exposures of less than a second. By floating the optical table with approximately 85 psi of nitrogen in the six pneumatic supports, the transmitted building vibration is reduced, resulting in less than 6% of a full fringe depth instability. This corresponds to a near 10 times improvement in fringe stability.

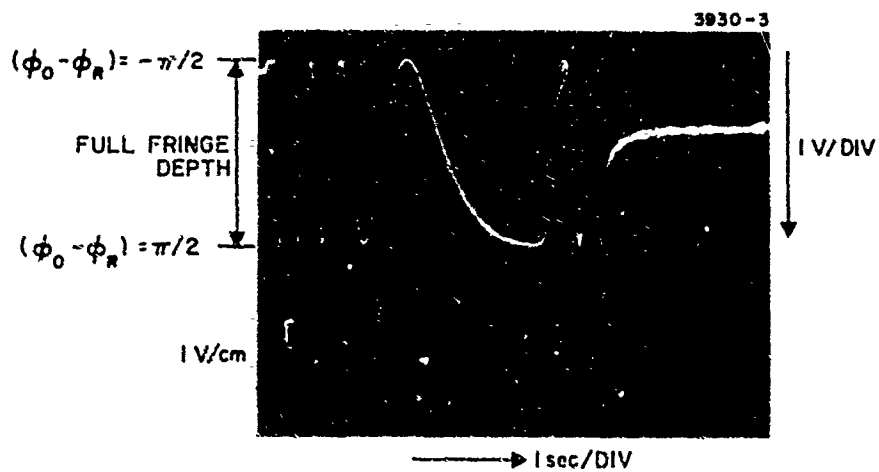


Fig. 22. Full fringe depth corresponding to a  $\lambda/2$  relative path length shift.

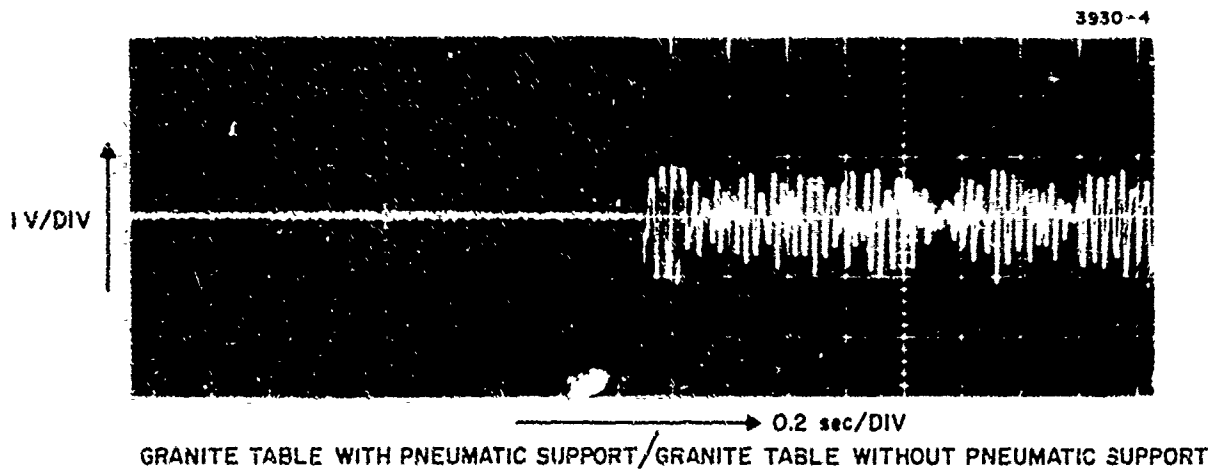


Fig. 23. Vibration isolation, pneumatic mounts improve fringe stability by 10 times.

The acoustic enclosure was tested by induced acoustical noise from an audio-oscillator and speaker placed near the acoustic shield. At 120 Hz, near the first order torsional bending frequency of the granite surface, fringe instability of 54% of a full fringe depth was observed without the shield. For a corresponding disturbance, the acoustic shield completely attenuates the high frequency acoustical disturbance, as shown in Fig. 24. Other high frequency acoustical noises at frequencies greater than 100 Hz were also effectively attenuated. Frequencies less than 100 Hz can only be attenuated by the addition of more mass to the acoustic shield, which would consequently reduce the effectiveness of the optical table and pneumatic supports by raising the center of gravity.

The interferometer phase detector was a useful tool in assembling the construction hardware, since many fringe instabilities result from vibrating optical mounts. Many iterative improvements in construction hardware stability were made by noting improved fringe stability by the addition of supporting mounts such as those found on the tall vertical beam steering units.

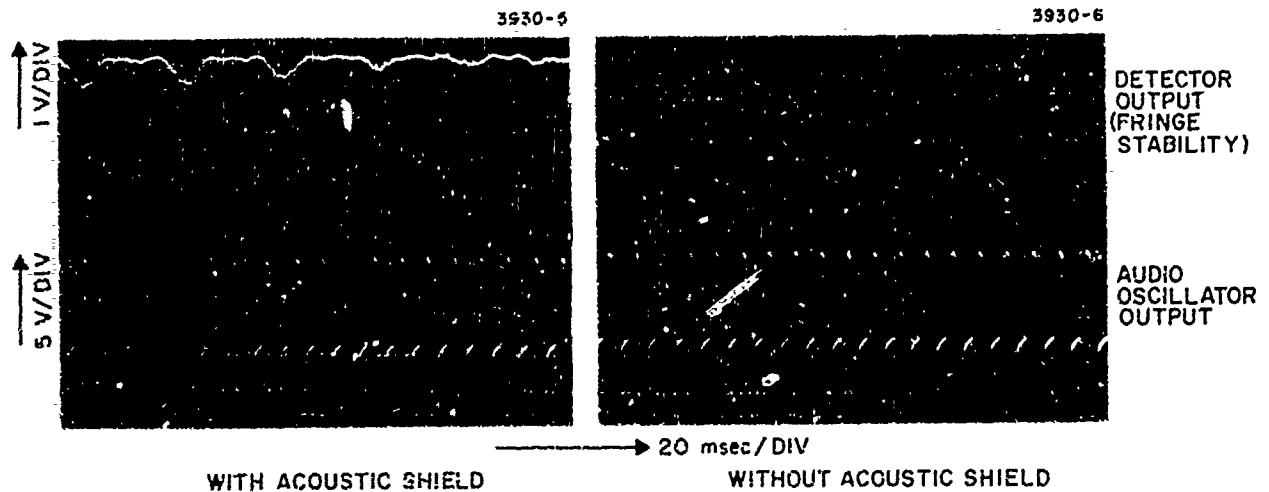


Fig. 24. High frequency acoustical noise at 126 Hz, the first order torsional bending frequency of the granite surface, is attenuated by the acoustic shield.

Figure 25 shows the fringe stability of the recording apparatus with environmental isolation. The full fringe depth is calibrated at the end of the trace. Notice the phase sensitivity improvement as the trace is near the midpoint of a full fringe depth, where small relative phase difference perturbations can cause large fringe intensity jumps due to the sinusoidal intensity variation of a fringe with respect to linear variation of phase difference. Although the fringe stability is relatively good due to the stability of construction hardware design and environmental isolation, long time hologram lens exposures would suffer efficiency loss due to the fringe drift resulting from thermal effects of the recording beam on optical elements and mounts.

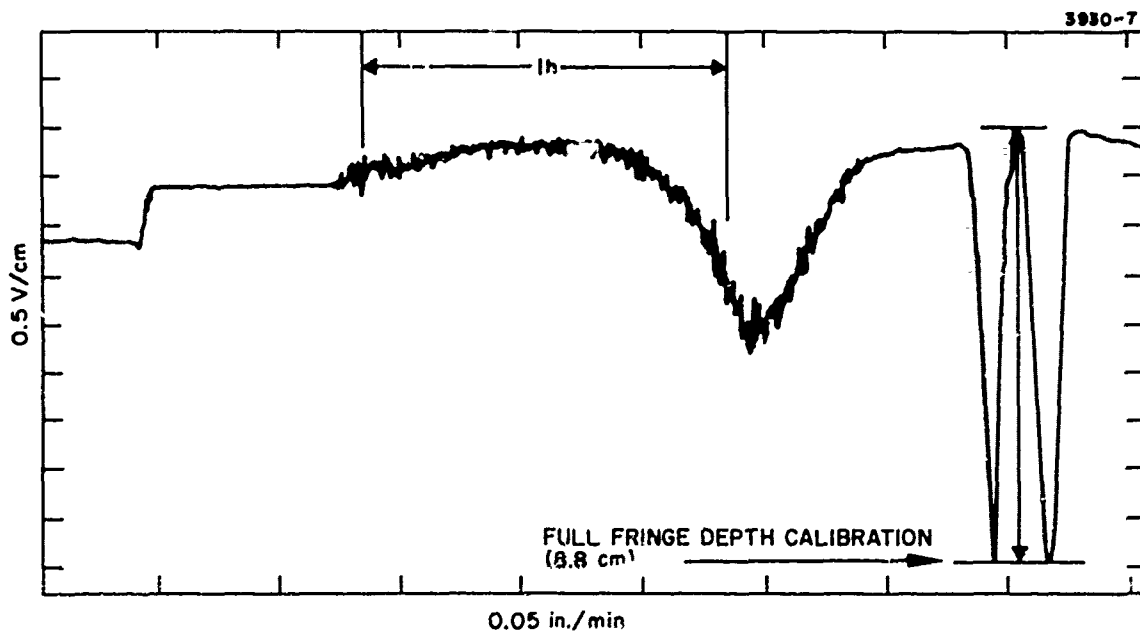


Fig. 25. Experimental evaluation of the full-scale hologram recording apparatus without fringe control exhibits good short term stability.

## V. Performance Evaluation.

### 3. FRINGE CONTROL SYSTEM—LONG TERM FRINGE STABILITY

The fringe control system locks the relative phase of the object and reference beams in the recording apparatus to maintain  $\lambda/22$  fringe stability over the 1 to 2 hours (maximum) required to record high-efficiency, large-aperture hologram lenses.

The long-term fringe instability due to thermal changes in optical elements and mounts is corrected by the fringe stabilizing control system. The system consists of integrating the difference output of the phase detectors until a balanced fringe intensity at the middle of a full fringe depth, the most phase sensitive location, is maintained by a piezoelectric translator actively correcting the relative phase variation between the two construction beams.

Figure 26 shows the noise of the photodetector amplifiers with no input and shows the amplifiers with the dark current noise of the photodetectors. In both cases, the noise level is very low compared to signal levels corresponding to a full fringe depth; typically four or more volts swing corresponding to maximum to minimum fringe intensity swing. The signal-to-noise ratio for a  $\lambda/2$  phase shift is 40. These low noise levels, achieved for current-to-voltage gains of  $44 \times 10^6$  ensure accurate detection of phase instability in the recording apparatus.

Figure 27 shows the ability of the fringe control system to lock the relative phase of the recording beams for over two hours. The straight horizontal line is one of the detectors' output, which remains stable in the midpoint of a full fringe depth. A trace of the other detector, which is  $180^\circ$  out of phase, would show a similar horizontal line at the midpoint of the full fringe depth since that is the only intensity location where the two detectors can be balanced. Any phase perturbations cause an effective phase error signal, which is integrated and consequently corrected by the piezoelectric translator until the detectors are balanced, thereby locking the phase of the two construction beams.

The corresponding sloping trace is the integrator output, which is amplified 10 times to translate the piezoelectric translator in the object construction beam to correct for phase drift between the two construction beams. Thus, excellent phase stability over an approximate two hour period was achieved by the fringe control system. The integration output change of 8 V during the two hour period was 40% of its dynamic range. This indicates an effective stabilization period for the recording apparatus of over 4 hours, compared to a maximum anticipated exposure period of 2 hours. The oscilloscope photo of a small section of the fringe stability trace shows the true amplitudes of the high frequencies because the preamplifiers of the strip chart recorder attenuates at 3 dB per octave. The remaining high frequency jitter is less than 9% of a full fringe depth, calibrated at the end of the trace. This 9% of a full fringe depth corresponds to a  $\lambda/22$  phase error. Therefore, the long term fringe stability required for 1 to 2 hours exposure of the large aperture HUD hologram lens is achieved with the fringe control system. This long term stability ensures high contrast interference fringe recording and, therefore, high efficiency hologram lenses.

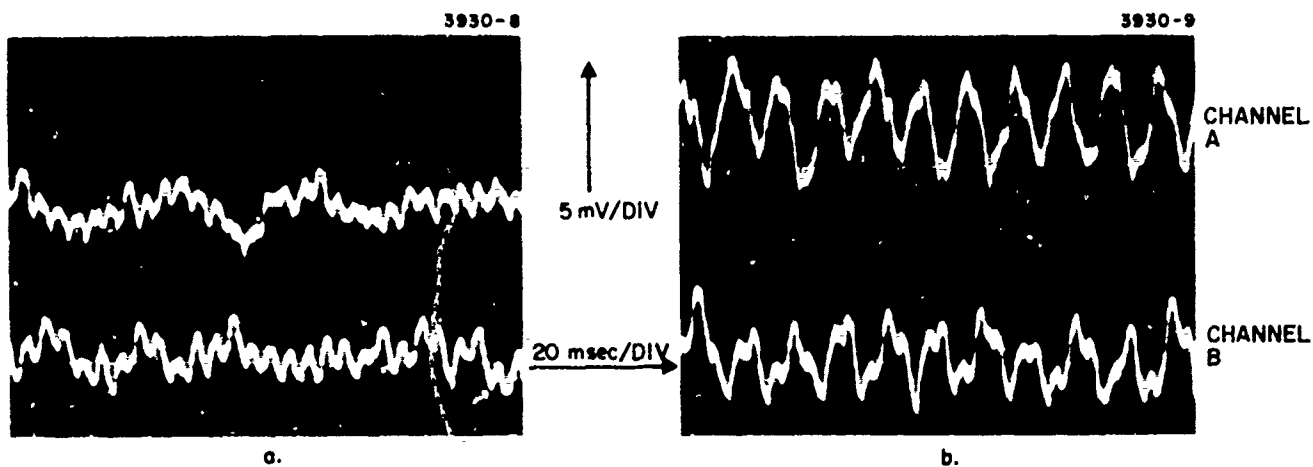


Fig. 26. Low amplifier noise, with no input (a) and dark current input of the photo-detectors (b), for current to voltage gains of  $44 \times 10^6$ .

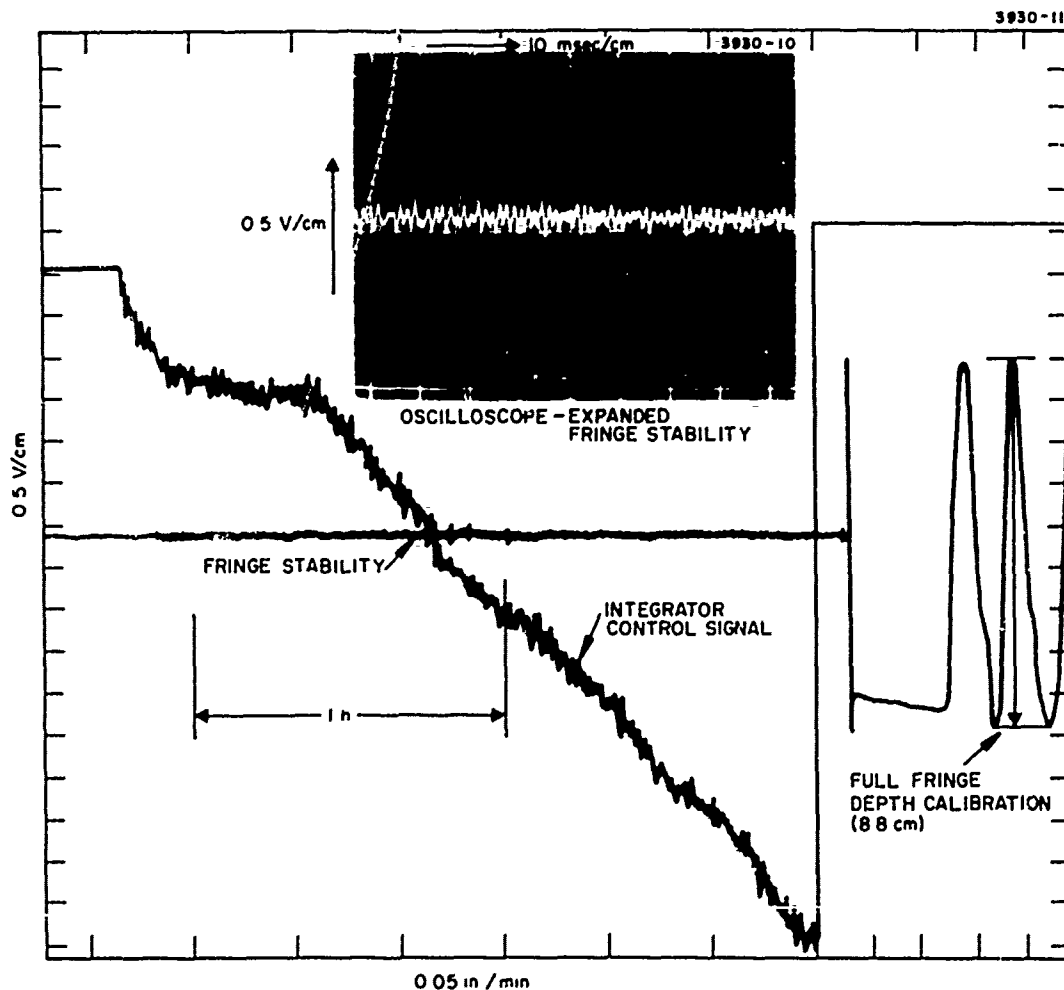


Fig. 27. Experimental evaluation of the full-scale recording system show that  $\lambda/22$  fringe stability for two hours is maintained by the active fringe control system.

## VI. Processing Equipment Design

### 1. DRYING CHAMBER AND AGITATION TANK DESIGN

A circulation drying chamber and nitrogen-burst agitation tanks were designed for uniform processing of 18 in. x 18 in. holographic plates, to enhance reproducibility of high quality, uniform large aperture HUD hologram lenses.

The processing of dye-sensitized dichromated gelatin was developed and optimized in Phase 1, Contract N62269-73-C-0388 and is described in detail in Section IV, "Red-Sensitive Recording Material Development," of the final report<sup>2</sup> covering that contract. The silver must be removed from the 18 in. x 18 in. x 0.25 in. Kodak 649F plates before the emulsion is dye-sensitized, dichromated and dried, to be used to expose the large aperture hologram lens in the recording apparatus. After exposing, the holographic plate must be agitated in 1 M triethanolamine and four increasing 25% steps of concentration of 2-isopropanol before it is dried in a nitrogen atmosphere. During all the processing steps, uniform drying at proper relative humidity and temperature, uniform agitation in processing baths, and minimum exposure to dust are vital to enhance reproducibility of high quality, uniform hologram lenses. Mr. Andrejs Graube, member of the Technical Staff at Hughes Research Laboratories, designed processing equipment based on the previous material development and optimization of dye sensitized dichromated gelatin processing.<sup>7</sup>

A standard photographic tank with nitrogen agitation can be used to remove silver halide from the photographic emulsion and to properly harden the gelatin layer. During the sensitizing step, the holographic plates are immersed in the dye solution. After sensitizing, the plates must be dried at a uniform drying rate over the emulsion surface to ensure uniform sensitization of the emulsion layer. Figure 28 shows the drying chamber design to ensure uniform drying at 40% relative humidity. The 40% relative humidity is obtained using  $\text{CaCl}_2$  solution, with a circulating fan to ensure uniform humidity within the drying chamber. A diffused air flow on the emulsion surface dries the gelatin layer at a uniform rate to obtain optimum sensitization of the holographic emulsion.

Post-exposure processing requires nitrogen burst agitation of the exposed holographic plate to obtain process control and reproducibility in processing large aperture hologram lenses. The agitation tank design, shown in Fig. 29, incorporates nitrogen burst through a fritted glass tubing to promote uniform swelling and dehydration of the holographic emulsion as the plate goes through various process baths. The arrangement of the processing tank table minimizes exposure to dust during travel between processing tanks. A nitrogen atmosphere chamber placed over the last, 100% isopropanol, agitation tank allows the holographic plate to be raised directly into a zero relative humidity

atmosphere for drying without exposure to dust or the surrounding environment.

These processing equipment designs were based on experience in optimizing the dye-sensitized dichromated gelatin, achieved in the Phase I contract and on experience in processing obtained in other hologram optics developments such as the helmet-mounted hologram lens display.<sup>4</sup> The design goals for uniform drying and agitation are applicable to all types of hologram processing, reflection or transmission holograms, where high process control is needed for high quality hologram lenses.

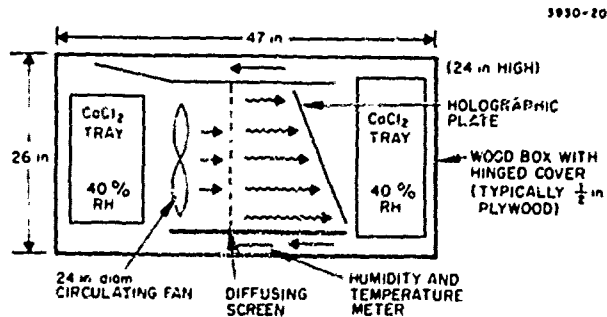


Fig. 28. Drying chamber designed to ensure uniform drying of 18 in. x 18 in. holographic plates.

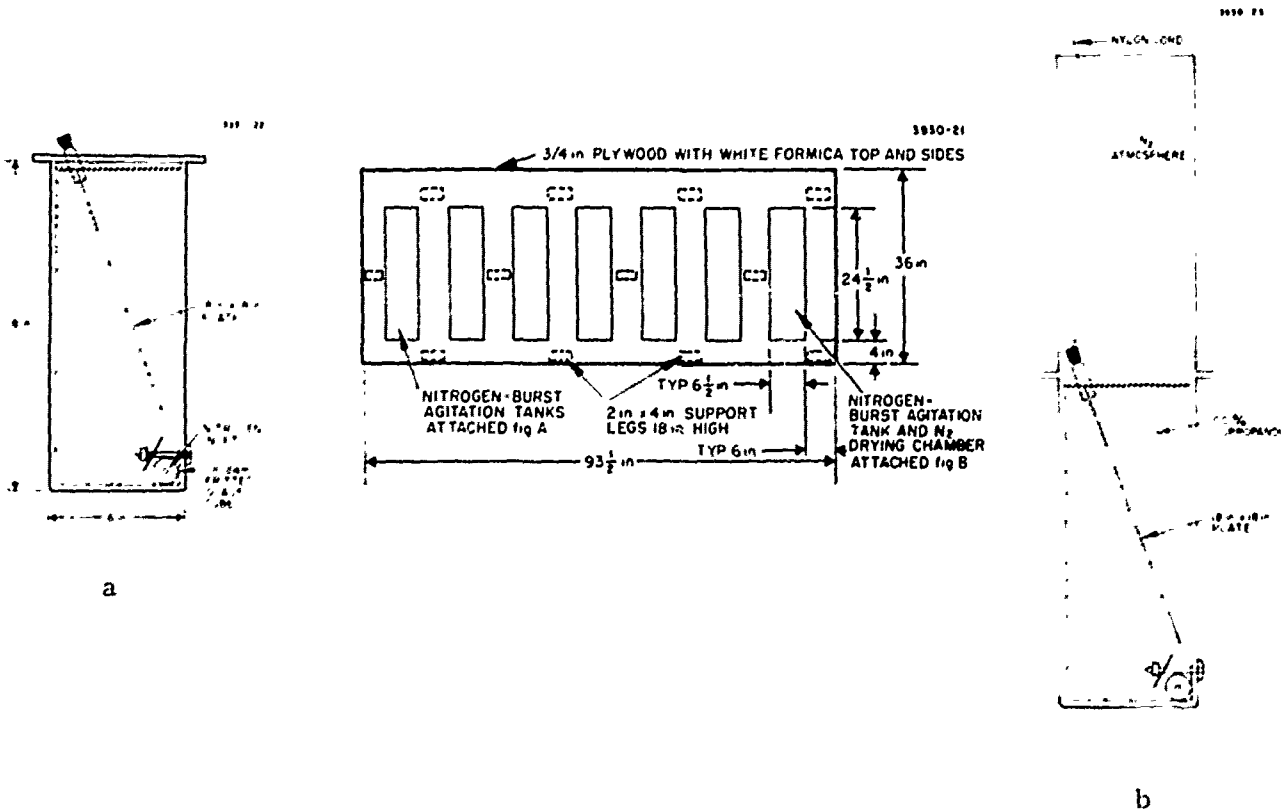


Fig. 29. Processing tank table with nitrogen-burst agitation tanks.

## REFERENCES

1. "Specification of Hologram Lens System," Naval Air Development Center, Air Vehicle Technology Department (20 November 1972).
2. Final Technical Report for period 2 April 1973 - 1 April 1974, Contract N62269-73-C-0388, "Holographic Lens for Pilot's Head-Up Display," prepared for Naval Air Development Center, Warminster, Pennsylvania 18974, by Hughes Research Laboratories, Malibu, California 90265, D.H. Close, A. Au, A. Graube (August 1974).
3. G. E. Moss, "Wide-Angle Holographic Lens for a Display System," J. Opt. Soc. Am. 64, 552A (April 1974).
4. Contract F33615-73-C-4110, from the Aerospace Medical Research Laboratory, Wright-Patterson AFB, "Holographic Visor Helmet Mounted Display," Final Report not yet available.
5. R. J. Collier, C. B. Burckhardt, and L. H. Lin, Optical Holography (Academic Press, New York, 1971).
6. D. Neumann and H. W. Rose, "Improvement of Recorded Holographic Fringes by Feedback Control," Applied Optics, Vol. 6, Number 6, 1097-1104, (June 1967).
7. A. Graube, "Hologram Recording with Red Light in Dye-Sensitized Dichromated Gelatin," Optics Communication, Vol. 8, Number 3, 251-253, (July 1973).